# High Temperature Mercury Oxidation Kinetics via Bromine Mechanisms

By

Terumi Okano

A Thesis

Submitted to the Faculty

of the

WORCESTER POLYTECHNIC INSTITUTE

in partial fulfillment of the requirements for the

Degree of Master of Science

in

Chemical Engineering

May 2009

APPROVED:

Dr. Jennifer Wilcox, Major Advisor

_____

Dr. David DiBiasio, Head of Department

_____

# Abstract

As the foremost production of electricity in the United State comes from coal-fired plants, there is much more to learn on the topic of mercury which is a common component in coal. The speciation of mercury in the flue gas determines the best control technology for a given system. Because of the difficulty in measuring mercury at different stages of the process, it is practical to use mercury reaction kinetics to theoretically determine mercury speciation based upon coal composition, plant equipment and operating conditions.

Elemental mercury cannot be captured in wet scrubbers; however, its oxidized forms can. Chlorine is a reasonable oxidizing agent and is naturally found in bituminous coal, but bromine is an even better oxidizing agent because of its larger size, it has stronger London dispersion force interactions with mercury. Bromine additive technologies have recently been implemented in several companies to enhance mercury oxidation. Because capture technologies are highly dependent upon the form of mercury that is present, investigations into their speciation are extremely important.

Though there have been numerous efforts to study mercury compounds as relevant to atmospheric studies, there is little data currently available for mercury compounds found in combustion flue gases. It would be particularly beneficial to obtain kinetic rate constants at various high temperature and pressure conditions typical for a combustion system. Prevalent species of mercury containing bromine in coal combustion flue gases were studied using density functional theory (DFT) and a broad range of *ab initio* methods. Reaction enthalpies, equilibrium bond distances, and vibrational frequencies were all predicted using DFT as well as coupled cluster (CC) methods. All electronic calculations were carried out using the Gaussian03 or MOLPRO software programs.

Kinetic predictions of three first-stage and three second-stage oxidation reactions involving the formation of oxidized mercury via bromine containing compounds are presented. Understanding the speciation of mercury in the flue gases of coal combustion is paramount in developing efficient technologies to ensure its capture.

# Acknowledgements

The completion of this work required a number of individuals and groups to contribute invaluable assistance. The following is a list of those whom deserve to be recognized for their efforts:

Thesis Advisor:
Dr. Jennifer Wilcox

Lab Mates:
Erdem Sasmaz and Bihter Padak

Department Administrative Assistants:
Felicia Vidito, Tiffany Royal, and Sandra Natale

Technical Assistance:
Stanford Center for Computational Earth & Environmental Science (CEES)

In addition, thanks go out to all the Chemical Engineering faculty, students, and staff for their support.

# Table of Contents

# List of Figures

# List of Tables

# Chapter 1: Introduction to Mercury Reaction Kinetics

The release of the toxic trace metal, mercury (Hg), has long been a significant issue for coal-fired power plants which must modify their post-processing systems to capture mercury from their combustion flue gases. Unlike its oxidized forms, $Hg^{2+}$ and $Hg^{+}$, elemental mercury cannot be captured in wet scrubbers. Chlorine is a strong oxidizing agent and is naturally found in bituminous coal, but bromine is an even better oxidizing agent because of its larger size, which increases its polarizability resulting in a stronger electronic interaction with mercury through their London dispersion forces. This has been shown through fairly recent experiments carried out on the pilot-scale and short-term full-scale by the US Department of Energy on the oxidation of mercury by chlorine and bromine compounds.[1] Other field studies have shown bromine to be effective in mercury removal from coal-fired boilers and a bromine additive technology has recently been implemented in several companies to enhance mercury oxidation.[2] In addition, it has recently been shown that direct bromine gas injection can effectively convert elemental mercury to oxidized mercury.[3] Since capture technologies are highly dependent upon the form of mercury that is present, investigations regarding their speciation are extremely important. Understanding the kinetic and thermodynamic behavior of mercury from the high to low temperature regime will allow for increased model accuracy in predicting mercury's complicated speciation, which in turn will facilitate the design and application of more effective mercury control devices. More specifically, these rate data can be used in the creation of a mercury-bromine mechanism that currently does not exist for combustion environment applications.

The growing interest in mercury capture from coal-fired plants comes from recent regulations. The Clean Air Mercury Rule (CAMR) was aimed at placing a cap on mercury emissions and reducing current levels by 70 percent by the year 2018.[4] It is possible that the government at the state level will take the initiative to make up their own state-wide regulations which may be stricter than those originally provided in CAMR. Therefore, the interest in mercury capture remains strong.

Though there have been numerous efforts to study mercury compounds as relevant to atmospheric studies, there is little data currently available for mercury compounds found in combustion flue gases. Experimentally- and theoretically-derived rate data available in the literature for modeling mercury-chlorine reactions at combustion conditions are limited. This warrants a kinetic study which can be appropriately performed using computational chemistry methods. This paper presents an *ab initio* study of three first-stage oxidation reactions and three second stage oxidation reactions of mercury with bromine and hydrogen compounds likely present in coal furnace flue gases.

First-stage oxidation reactions:

$$Hg + Br \rightarrow HgBr \quad (1)$$
$$Hg + Br_2 \rightarrow HgBr + Br \quad (2)$$
$$Hg + HBr \rightarrow HgBr + H \quad (3)$$

Second stage oxidation reactions:

$$HgBr + Br \rightarrow HgBr_2 \quad (4)$$
$$HgBr + Br_2 \rightarrow HgBr_2 + Br \quad (5)$$
$$HgBr + HBr \rightarrow HgBr_2 + H \quad (6)$$

Kinetic parameters for forward and reverse reactions for a temperature range of 298.15 – 2000 K at atmospheric pressure are obtained using TST for the four single displacement reactions and RRKM theory for the two recombination reactions. Additionally, for reactions without experimental or theoretical values to compare against, the hard sphere collision model was used to calculate the rate constant to set an upper bound for TST.

## Chapter 2: A Brief Review of Mercury Air Pollution Control

Before delving into mercury reaction kinetics, it is important to recognize the role kinetics plays in understanding mercury pollution control from coal-fired plants. The form or speciation of mercury in the flue gas greatly affects the ways in which it can be captured. It is possible to measure mercury at different stages of the process, but the current measurement methods only allow for the direct measurement of oxidized forms and so are more qualitative than quantitative. Because of this, it is practical to use mercury reaction kinetics to theoretically determine mercury speciation based upon coal composition in addition to plant equipment and operating conditions.

It is common to find mercury compounds in coal and when the coal is burned, some of it is released into the atmosphere. In 1999, it was estimated that 64% of mercury going into the boiler was emitted from coal fired plants in the US.[5] There exist different control strategies dependent upon the form of mercury. There are three different forms of mercury: elemental ($Hg^0$), particulate ($Hg^P$), and oxidized ($Hg^{1+}$, $Hg^{2+}$). The coal properties that most affect mercury speciation in the flue gas are coal rank and the concentration of chlorine and sulfur in the coal.[6] Higher amounts of chlorine in bituminous coals are believed to oxidize mercury, mostly to mercury(II) chloride ($HgCl_2$). Subbituminous coal or lignite, with lower or little chlorine content, tend to have relatively low concentrations of oxidized mercury. As far as halogens are concerned, chlorine has the greatest effect on mercury, but bromine also plays a role in mercury oxidation. Sulfur decreases mercury capture ability in air pollution control devices; there has been some speculation as to the reason for this but controversy still exists. Regardless of the type of coal, mercury is in the gaseous form, $Hg^0$, in the high temperature

(~1600˚F) region of the coal-fired boilers. As the gas cools, mercury undergoes homogeneous and heterogeneous transformations which are highly dependent upon flue gas composition and quench rate, as well as the fly ash quantity and its properties. The heterogeneous pathway is found to be dominant over the homogeneous pathway; even so, it is important to study the homogeneous pathway because it does occur to some extent and has an affect on the final outcome of mercury speciation in the flue gas.[6] This paper focuses on only the homogenous pathway.

The uniqueness of each plant contributes to the complication of the many factors that make it difficult to predict mercury behavior in the coal-fired systems. Particulate and oxidized mercury are the easiest forms to capture and can be captured with some currently existing air pollution control technologies. Mercury bound to particulates, for example, can be removed by an electrostatic precipitator, fabric filter, or a particle scrubber. Because all of these are already designed to efficiently remove particulate matter, mercury is automatically removed as well. Some oxidized mercury can be removed with technology such as a flue gas desulfurization or a spray dryer adsorber system; these are designed to remove sulfur but can also remove mercury for some types of coal. There are technologies specific to mercury capture, such as bromine gas and activated carbon injection that attempt to form either $Hg^P$ or $Hg^{2+}$.

In addition, the type of coal burned has a huge impact on what kind of air pollution control device will be most effective to capture mercury. This is because of the importance in knowing the forms of mercury needing to be captured. The coal type determines the components found in the flue gas released during coal combustion so the main concern is the

different species mercury is interacting with in the flue gas. To study these interactions, it is necessary to know the kinetics of the reactions occurring. Chemical kinetics is the study of reaction rates and is affected by temperature, pressure, and physical state. All of the reactions studied here are at atmospheric pressure and in the gas phase. Therefore, the kinetics are affected only by a temperature dependence as shown in the Arrhenius equation (7) below.

$$k = Ae^{-E_a / RT} \qquad (7)$$

The rate constant, $k$, is determined by finding the activation energy, $E_a$, and the pre-exponential factor, $A$. The ideal gas constant is $R$ and $T$ is the temperature. The activation energy is the energy difference between that of the activated complex and the sum of the ground state energies of the reactant species. The pre-exponential factor is defined as an empirical factor relating temperature to the rate constant. It can be calculated through quantum mechanics using the partition functions of the reactants, activated complex, and products.

The quantum mechanics, the thermodynamics (derived from knowledge of the wave function) and ground state energies are solved using either Gaussian03[7] and/or MOLPRO.[8] Both of these programs use the same basic principles of solving the electronic Schrödinger equation to find the electronic energy for a particular nuclear configuration. Because the Schrödinger equation cannot easily be solved exactly for systems larger than the hydrogen atom, the program uses a wave function represented by finite basis sets to simplify the calculation into an algebraic equation which can then be solved using numerical methods. Using the electronic energies, a potential energy surface can be constructed to find the

activated complex for a particular reaction. The activated complex, also called a transition state, is a configuration of atoms at the highest energy point along the reaction coordinate. The energy difference between the reactant and the activated complex is the activation energy. Once the activated complex is found, Transition State Theory (TST) for bimolecular reactions or Rice-Ramsperger-Kassel-Marcus (RRKM)[9] Theory for unimolecular reactions can be used to calculate the reaction kinetics. Gaussian and MOLPRO also solve for partition functions, vibrational frequencies, and thermodynamics, all of which are used within both kinetic frameworks to determine the gas-phase kinetics for any reaction.

# Chapter 3: Literature Review on Mercury-Bromine Kinetics

## *3.1 Theoretical & experimental thermodynamic data on Hg-Br kinetics*

Though there have been numerous efforts to study mercury-bromine compounds as relevant to atmospheric studies, there is little data currently available for these compounds found in combustion flue gases. It would be particularly beneficial to obtain kinetic rate constants at various high temperature and pressure conditions typical for a combustion system. This warrants a kinetic study which can be appropriately performed using computational chemistry methods. However, prior to evaluating mercury speciation predictions, all available experimental data must be compared to theoretical models to determine a best level of theory with which to move forward. An extensive *ab initio* study of several mercury-bromine compounds typically found in coal furnace flue gases has been conducted. Whenever possible, a comparison is made between experimental data and the theoretically-calculated geometries and vibrational frequencies. Additionally, reaction enthalpies are calculated for a collection of reactions involving these species using theoretical Gaussian total energies and experimental reaction enthalpies found using the enthalpies of formation of each compound.

Experimental geometries have been determined for many of the species mentioned. Researchers have employed a number of experimental techniques including electron diffraction ($HgBr_2$),[11] and Fourier Transform Spectroscopy ($Br_2$)[12] to predict structural properties of these compounds. Experimental methods have yielded typical bond length values of 1.41-2.28 Å for small diatomic molecules containing bromine and 2.23-2.62 Å for

mercury and bromides. There is some dispute over the linearity of $HgBr_2$, as Givan's[13] experiments clearly indicate nonlinearity; thus far, all of the limited theoretical calculations indicate linear or nearly linear geometries.[14,15] There does not seem to be any reliable data available for the bond length of HgBr, so the best available theoretical bond length of 2.494 Å[16] is used for comparison.

Unlike the geometric data, spectroscopic data exists for all of the compounds investigated. Several sources provided vibrational spectroscopy data for compounds $Br_2$,[12,17] HBr,[18] HgBr,[19] and $HgBr_2$.[20-22] Although experimental data is available for all of these species, the mode of vibration is not always specified.

The enthalpies of formation of simple mercury-bromine compounds have been examined in experimental studies and are reported by Chase[23] (HgBr and $HgBr_2$) and Cox (HBr).[24]. Limited theoretical work has also been carried out to determine the total energies of a few of these species along with enthalpies of reaction for several mercury-bromine reactions.[25] While no direct comparison between formation enthalpy and total energy can be made, the energy differences resulting from a reaction may be directly compared to one another. To this end, the accuracy of computational levels of theory in predicting the enthalpies of selected reactions can be evaluated against the available experimental data.

One other thermodynamic data of use is the reaction equilibrium constant. Reaction equilibrium constants can be used to perform a stability analysis for mercury-bromine reactions. From knowledge of the thermodynamic stability of the compounds through

studying the formation pathways, insignificant reactions can be set apart from those that may play a more crucial role in a given compound's formation. This aids in guiding the mercury-bromine reaction research for the purposes of coal combustion mercury reaction kinetics.

### *3.2 Theoretical & experimental kinetic data on Hg-Br kinetics*

Applications of previous kinetic investigations on bromine-oxidized mercury species have primarily dealt with the cycling of mercury within the atmosphere. Although the previous studies are very thorough, they do not give an indication of mercury oxidation behavior at the high-temperature conditions of coal combustion. The experimental and theoretical studies of mercury oxidation via bromine species have focused mainly on atmospheric conditions. There has been limited research carried out on bromine. Specifically, there are five reactions relevant to these studies that have previously determined rate constants. Only the following three reactions have experimentally determined rate constants:

$$Hg + Br \rightarrow HgBr, \quad (1)$$

$$Hg + Br_2 \rightarrow HgBr_2, \quad (8)$$

$$Hg + BrO \rightarrow HgBr + O \quad (9)$$

and the following reactions in addition to reactions (1) and (8), have theoretically determined rate constants:

$$Hg + Br_2 \rightarrow HgBr + Br \quad (2)$$

$$HgBr + Br \rightarrow HgBr_2, \quad (4)$$

In the current work, oxygen has not been included in any of the reactions, therefore reaction (9) has not been studied. For reaction (8), the kinetics were omitted on the basis that it has an extremely high activation energy due to the necessity of forming a triangular transition structure making it highly unlikely that mercury would follow this path to form $HgBr_2$. Reactions (1) and (2) can be found in the list of first-stage mercury oxidation reactions.

Of all six reactions studied, experimental kinetic parameters are available only for reaction (1).[26-29] Three of these experiments were conducted only at room temperature and the highest temperature at which the parameters were calculated was not much higher, at 448K. Reaction (1) has been calculated theoretically by Khalizov,[30] Goodsite,[31] and Shepler[16] and Reaction (2) by Balabanov.[32] Khalizov[30] used Canonical Variational Transition State Theory[33] to calculate the rate parameters, but only at the high-pressure limit; Goodsite[31] used RRKM Theory along with the hybrid density functional/Hartree-Fock B3LYP[34,35] method between a temperature range of 180-400K. Shepler[16] calculated kinetic parameters from quasiclassical trajectories and, unlike the other theoretical calculations, used argon as the bath gas. The current work employs RRKM theory at the CCSD(T)/Aug-cc-pVTZ level of theory with argon as the bath gas to calculate the temperature-dependent kinetic parameters for recombination reaction (1). It is distinctive that none of these reactions have rates calculated over the full temperature range typical for coal combustion systems. Balabanov,[32] for reaction (2), used the internally contracted multireference configuration interaction (singles and doubles) method with the augmented correlation consistent basis sets, aug-cc-

pV*n*Z-PP for calculating the reaction rates. As far as the author knows, there have been no experimental or theoretical calculations for reaction (2).

Experimental kinetic parameters are not available for reactions (4) through (6). However, reaction (4) has been calculated theoretically by Goodsite[31] and Balabanov.[32] Goodsite used Rice- Ramsperger-Kassel-Marcus (RRKM) Theory along with the B3LYP method to calculate reaction rates between the temperatures of 180-400K. Balabanov calculated kinetic parameters from quasiclassical trajectories and used the internally contracted multireference configuration interaction (singles and doubles) method with the multireference Davidson correction (icMCRI+Q)[36-40] combined with the augmented correlation consistent basis sets, aug-cc-pV*n*Z-PP ($n$ = 2, 3, 4) at the complete basis set limit.[32] It is worth noting that these authors have calculated the reaction rates up to 400K, which is far from the temperatures typical for coal combustion systems (298 – 2000K). To the author's knowledge, there has not been any prior study on the kinetics of reactions (5) and (6).

## Chapter 4: Why Study Mercury-Bromine Kinetics?

Determining the kinetics and reaction pathway for homogeneous mercury-bromine reactions in coal combustion flue gas will help to create a complete combustion model in CHEMKIN for mercury air pollution control strategy development. To work towards this, *ab initio* methods were adopted to examine a cost-effective way to determine mercury-bromine kinetics. It is a challenge to model these reactions due to the very large size of the mercury atom. Modeling comes at a high computational cost with limited accuracy due to the relativistic effects that become important when dealing with large molecules. A balance of time and accuracy was necessary to effectively determine the reaction kinetics.

Though mercury is of great concern, especially for power plants that would like to reduce their emissions of this trace metal, there is surprisingly little information on the kinetics at high temperatures, i.e., at typical combustion conditions. The six reactions studied strictly consist of mercury, bromine, and hydrogen atoms, and result in three first-stage oxidation and three second-stage oxidation reactions. These reactions were chosen because they are likely to occur along the way toward the complete mercury oxidation compound ($HgBr_2$).

A thorough literature search, as stated in section 3, revealed that numerous rate studies had been completed on the HgBr recombination reaction, i.e., reaction (1), but very little was found on the other four reactions. In addition, none of the studies reported calculated rates at high temperatures, which is necessary for the modeling of combustion systems. Elucidating the kinetics for these six reactions would greatly improve mercury capture predictions for systems with mercury-bromine technologies. Much more accurate predictions could be made,

drastically reducing the necessity of monitoring and experimental testing for mercury, which is in many cases a qualitative approach for combustion systems.

# Chapter 5: Theory and Methodology

## *5.1 Method and Basis Set Selection*

### *5.1.1 First-Stage Mercury Oxidation Reactions*

Before the kinetic and equilibrium parameters could be calculated, it was necessary to determine which level of theory would be the most accurate for the mercury compounds by comparing geometries, vibrational frequencies, and thermochemical parameters to experimental data. The B3LYP method was used with two basis sets. The first basis set employed was LANL2DZ[41], which uses an all-electron description for atoms of the first row elements, and an ECP for inner electrons combined with double-ς quality functions for the valence electrons for heavier atoms of elements such as mercury. The second basis set employs a relativistic compact effective potential, RCEP60VDZ of the Stevens et al. group,[42] which replaces 60 of mercury's atomic core electrons, derived from numerical Dirac-Fock wavefunctions using an optimizing process based upon the energy-overlap functional. Energy-optimized (8s8p5d)/[4s4p3d] Gaussian-type double-ς quality *sp* and triple-ς quality *d* functions were used for mercury, with the triple-ς *d* functions essential for describing the orbital shape changes that exist with the *d* occupancy. An extended triple-ς Pople basis set, 6-311G*, including the addition of a single polarization function was used for bromine and hydrogen atoms in conjunction with the RCEP60VDZ basis set.

For CCSD(T), the augmented correlation consistent basis sets of triple-ζ quality (Aug-cc-pVTZ-PP, shortened to AVTZ) incorporating scalar relativistic effects[43,44] were employed

through the use of small-core relativistic pseudopotentials (PP)[45] for the inner electrons of mercury and bromine. The PPs used were adjusted using the four-component multi-configuration Dirac-Hartree-Fock (MCDHF) data to allow for simultaneous extraction of adjusted scalar-relativistic PPs and spin orbit (SO) potentials which provides the most accurate results to date. This same basis set was employed for hydrogen, but without a PP, as it is unnecessary for such a small molecule. These methods and basis sets are a representative sample of the wide range of results obtained from a combination of 15 methods and level of theories that were tested for accuracy.

Experimental geometries and experimental spectroscopic data have been determined for the following species: HgBr, HBr, and $Br_2$. The experimental and theoretical values are compared in Table 1. In Table 2, the accuracy of computational levels of theory in predicting the enthalpies of selected reactions are evaluated against the available experimental data.

**Table 1**. Comparison between experimental and theoretical vibrational frequencies, bond length, and entropies for molecules involved in reactions (1)-(3) for three level of theories. The theoretical values are expressed as deviations from experiment.

| **Vibrational Frequencies ($cm^{-1}$)** | | | | |
|---|---|---|---|---|
| | **Experiment** | **B3LYP/LANL2DZ** | **B3LYP/RCEP60VDZ** | **CCSD(T)/AVTZ** |
| **HBr** | 2650[a] | -249.75 | -107.92 | -5.59 |
| **$Br_2$** | 325.3[b] | -54.84 | -14.96 | -11.02 |
| **HgBr** | 188.3[c] | -21.83 | -34.43 | -25.60 |
| **Bond Length (Å)** | | | | |
| | **Experiment** | **B3LYP/LANL2DZ** | **B3LYP/RCEP60VDZ** | **CCSD(T)/AVTZ** |
| **HBr** | 1.41[d] | 0.05 | 0.02 | 0.01 |
| **$Br_2$** | 2.28[e] | 0.23 | 0.05 | 0.03 |
| **HgBr** | 2.49[f] | 0.29 | 0.15 | 0.05 |
| **Entropy (cal/mol)** | | | | |
| | **Experiment** | **B3LYP/LANL2DZ** | **B3LYP/RCEP60VDZ** | **CCSD(T)/AVTZ** |
| **HBr** | 47.46[g] | 0.08 | -0.01 | -0.02 |
| **$Br_2$** | 58.64[g] | 0.59 | 0.07 | 1.45 |
| **HgBr** | 64.86[h] | 1.17 | 0.83 | 0.39 |

[a]Reference 18. [b]Reference 12, 17. [c]Reference 19. [d]Reference 17, 46. [e]Reference 12,17. [f]Reference 51. [g]Reference 52. [h]Reference 23. The RCEP60VDZ basis set uses 6-311G* for the H and Br molecule.

**Table 2**. Comparison between experimental and theoretical reaction enthalpies (kcal/mol) for reactions (1) through (3) at three levels of theories. The theoretical values are expressed in kcal/mol as deviations from experiment.

| | Experiment[a] | B3LYP/LANL2DZ | B3LYP/RCEP60VDZ | CCSD(T)/AVTZ |
|---|---|---|---|---|
| **Hg + Br → HgBr** | -16.51 | -2.04 | -0.21 | 0.77 |
| **Hg + Br2 → HgBr + Br** | 29.56 | -18.27 | -0.73 | 2.03 |
| **Hg + HBr → HgBr + H** | 70.95 | -12.63 | -3.26 | 4.57 |

[a]Experimental data for mercury species from NIST[52]; data for other species taken from CODATA,[24] CRC,[53] and Wilmouth.[54] The RCEP60VDZ basis set uses 6-311G* for the H and Br molecule.

These tables reveal the best level of theory available to calculate the kinetics for each reaction. From Table 1 it can be seen that the CCSD(T)/AVTZ level of theory predicts bond distances, vibrational frequencies, and thermochemical data of the reaction species the best or at least a very close second best, with exception of one entropy value where it deviates less than 1.5 cal/mol. Therefore, for each individual species at this level of theory deviates the least from experimental data available in the literature. Table 2 also shows the CCSD(T)/AVTZ level of theory performs well, deviating at most by 5 kcal/mol. However, the B3LYP/RCEP60VDZ level of theory performs better for all three reactions in predicting the reaction enthalpies.

The B3LYP DFT method has been shown to perform well in certain cases, the results depending on the geometry and whether the molecule was charged or neutral; in this case of simple geometries and relatively large radical and neutral molecules, it has been found to perform well. Another study shows that B3LYP works well in predicting structures and energetics for small mercury complexes.[55] In this study, the author compares CCSD(T)

results with B3LYP for small $Hg^{IV}$ complexes and concludes that the energetics are best described using hybrid functionals like B3LYP as compared to SVWN5[56] and BP86[57,58].

The kinetics for reaction (1) were calculated at the CCSD(T) level of theory. This method was chosen due to its speed and sufficient accuracy in predicting geometries, vibrational frequencies, and thermochemical parameters compared to experiment, as highlighted in Table 1. Even though the reaction enthalpy is less accurate compared to B3LYP/RCEP60VDZ, the difference is less than 0.75 kcal/mol, and the accuracy in the other parameters warrants it to be the best level of theory in this case. The last two reactions used the B3LYP/RCEP60VDZ level of theory to calculate the kinetics as the energies of the reactants and activated complex are the most important parameters affecting the kinetics. The reaction enthalpies at this level of theory were an improvement of more than 1 kcal/mol compared to the CCSD(T) level of theory.

### *5.1.2 Second Stage Mercury Oxidation Reactions*

The same method was used to determine which level of theory would be the most accurate for mercury. The previously mentioned methods, B3LYP and CCSD(T), were utilized along with the same basis sets with exception of RCEP60VDZ being replaced by ECP60MDF.

Experimental geometries and experimental spectroscopic data were once again determined for the following species: $HgBr_2$, HgBr, HBr, and $Br_2$. The experimental and theoretical values are compared in Table 3. The enthalpies of formation of simple mercury

and bromine compounds have been examined and the resulting reaction enthalpies are evaluated against the available experimental data in Table 4.

**Table 3**. Differences between experimental and theoretical vibrational frequencies, bond length, and entropies for molecules involved in reactions (4)-(6) for three levels of theories. The theoretical values are expressed as deviations from the experimental values.

| Vibrational Frequencies ($cm^{-1}$) | | | | |
|---|---|---|---|---|
| | **Experiment** | **B3LYP/LANL2DZ** | **B3LYP/ECP60MDF** | **CCSD(T)/AVTZ** |
| **HBr** | 2650[a] | -250 | -108 | -5.59 |
| **$Br_2$** | 325.3[b] | -54.8 | -15.0 | -11.0 |
| **HgBr** | 188.3[c] | -46.9 | -21.8 | -25.6 |
| **$HgBr_2$** (symmetric stretch) | 218d | -40.2 | -16.6 | 0.25 |
| (bend) | 68e | -19.9 | -7.97 | -0.45 |
| (asymmetric stretch) | 293f | -49.2 | -21.4 | -3.40 |
| **Bond Length (Å)** | | | | |
| | **Experiment** | **B3LYP/LANL2DZ** | **B3LYP/ECP60MDF** | **CCSD(T)/AVTZ** |
| **HBr** | 1.41g | 0.05 | 0.02 | 0.01 |
| **$Br_2$** | 2.28b | 0.23 | 0.05 | 0.03 |
| **HgBr** | 2.49h | 0.29 | 0.12 | 0.05 |
| **$HgBr_2$** | 2.44i | 0.14 | 0.03 | -0.04 |
| **Entropy (cal/mol)** | | | | |
| | **Experiment** | **B3LYP/LANL2DZ** | **B3LYP/ECP60MDF** | **CCSD(T)/AVTZ** |
| **HBr** | 47.46j | 0.08 | -0.01 | -0.02 |
| **$Br_2$** | 58.64j | 0.59 | 0.07 | 1.45 |
| **HgBr** | 64.86k | 1.17 | 0.61 | 0.39 |
| **$HgBr_2$** | 76.48l | 0.40 | -1.09 | -8.96 |

[a]Reference 18. [b]Reference 12,17. [c]Reference 19. [d]Reference 20. [e]Reference 21. fReference 22. [g]Reference 17, 46. [h]Reference 51. [i]Reference 60. [j]Reference 53. [k]Reference 23. [l]Reference 22. The RCEP60VDZ basis set uses is 6-311G* for the H and Br molecule.

**Table 4**. Comparison between experimental and theoretical reaction enthalpies (kcal/mol) for reactions (4) through (6) at three levels of theories. The theoretical values are expressed in kcal/mol as deviations from experiment.

| | **Experiment[a]** | **B3LYP/LANL2DZ** | **B3LYP/ECP60MDF** | **CCSD(T)/AVTZ** |
|---|---|---|---|---|
| **$HgBr + Br \rightarrow HgBr_2$** | -72.02 | 18.29 | 1.89 | 0.08 |
| **$HgBr + Br_2 \rightarrow HgBr_2 + Br$** | -25.95 | 2.06 | 1.37 | 1.34 |
| **$HgBr + HBr \rightarrow HgBr_2 + H$** | 15.44 | 7.70 | -1.16 | 3.88 |

[a]Experimental data for mercury species from NIST[52]; data for other species taken from CODATA,[24] CRC,[53] and Wilmouth.[54] The ECP60MDF basis set uses is 6-311G* for the H and Br molecule.

These tables reveal the best level of theory to calculate the kinetics for each reaction. From Table 3 it can be seen that the CCSD(T)/AVTZ level of theory predicts bond distances, vibrational frequencies, and thermochemical data of the reaction species the best or at least a very close second best, with only one discrepancy, i.e., with a large deviation of 9 cal/mol from experiment for the entropy of $HgBr_2$. Therefore, each individual species at this level of theory deviates the least from experimental data available in the literature. Table 4 also shows the CCSD(T)/AVTZ level of theory overall performs the best, deviating at the most by 4 kcal/mol. However, the B3LYP/ECP60MDF level of theory performs better by over 2 kcal/mol for reaction (3). This is possibly because of the significant effect that the lack of accounting for spin orbit coupling and the lamb shift has at the CCSD(T) level of theory, as shown by Shepler.[16]

The CCSD(T) level of theory was used to calculate the kinetics for reaction (1) and (2). This method was chosen due to its speed and sufficient accuracy in geometry, vibrational frequency, and thermochemical predictions compared to experiment, as highlighted in Table 3. The B3LYP/RCEP60VDZ level of theory was the best choice to calculate the kinetics for reaction (3) because the reaction enthalpies at this level of theory were an improvement of more than 2 kcal/mol compared to the CCSD(T) level of theory. The accurate reaction enthalpy is more important than the accuracies of the individual molecules, in cases where the rest of the parameters are, in most cases, on the same order of accuracy. This is because the energies of the reactants and activated complex are very sensitive parameters directly affecting reaction kinetics through the activation energy term in the Arrhenius equation.

## *5.2 Theoretical Kinetic Methodology*

Kinetic and equilibrium parameters were evaluated over a temperature range of 298.15-2000K. In determining the rate constant for each reaction, the transition state theory equation (4) was modified with the tunneling correction factor of Wigner[61] (5) (where υ represents the single imaginary frequency value of the transition structure), so that the final rate constant value is given by equation (6).

$$k^{TST} = \frac{k_b T}{h} \frac{Q_{TS}}{Q_1 Q_2} e^{\left(\frac{-E_a}{RT}\right)} \tag{4}$$

$$k_T = 1 + \frac{1}{24}\left[\frac{hc\nu}{k_b T}\right]^2 \tag{5}$$

$$k = k^{TST} \cdot k_T \tag{6}$$

In the above equations, $k_b$ is Boltzmann's constant, $h$ is Plank's constant, $T$ is temperature, $E_a$ is the activation barrier, $R$ is the ideal gas constant, $Q_{TS}$, $Q_1$, $Q_2$ are the total partition functions of the transition structure and reaction species 1 and 2, respectively.

Additionally, the equilibrium constants for each reaction were calculated from equations (7) and (8). By determining the thermodynamic parameters of reaction enthalpy and entropy, the equilibrium curve as predicted both theoretically and experimentally could be compared, where all data existed.

$$K_{eq} = e^{\left(\frac{-\Delta G}{RT}\right)} \tag{7}$$

$$\Delta G = \Delta H - T\Delta S \tag{8}$$

In this way, an evaluation could be made of these quantities as well as the ratio of the rate constants to determine if the theoretical predictions, both kinetic and thermodynamic, matched existing experimental thermodynamic data.

# Chapter 6: Results and Discussion

## *6.1 First-Stage Mercury Oxidation Reactions*

### *6.1.1 Potential Energy Surfaces*

Potential energy curves and surfaces generated for reactions (1) through (3) are shown in Figure (1) through (3), respectively.

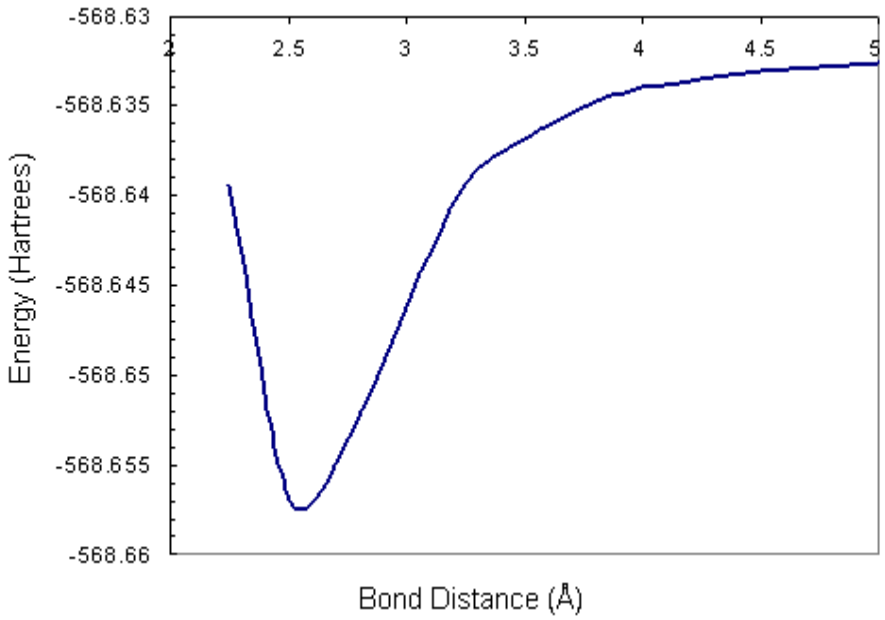


**Figure 1.** Reaction (1), HgBr recombination, potential energy curve at CCSD(T)/AVTZ level of theory.

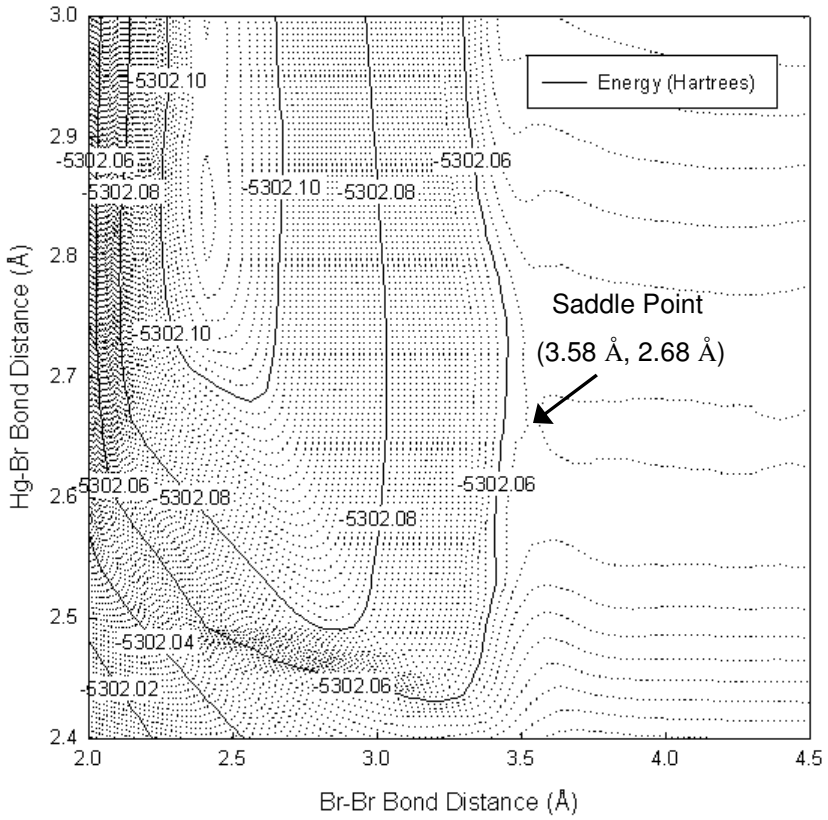


**Figure 2.** Reaction (2), Hg + $Br_2$ → HgBr + Br, potential energy surface at B3LYP/RCEP60VDZ level of theory.

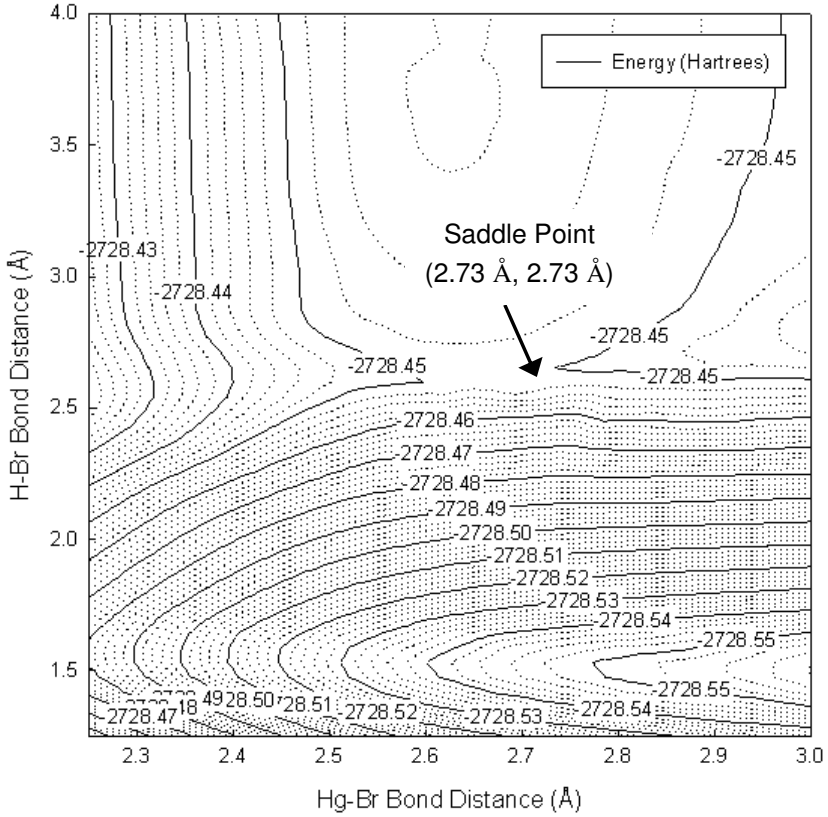


**Figure 3.** Reaction (3), Hg + HBr → HgBr + H, potential energy surface at B3LYP/RCEP60VDZ level of theory.

The Hg + Br recombination reaction potential energy curve was produced at the CCSD(T)/AVTZ level of theory. The curve is typical with the potential well representing the equilibrium energy between Hg and Br, i.e., the stable HgBr molecule. Unrestricted CCSD(T) was employed for the open-shell molecules in this reaction, which included all the single point energy calculations for the potential energy surface for reaction (1). The contour surfaces for reactions (2) and (3) were generated with approximately 200 single-point energy calculations at the B3LYP/RCEP60VDZ level of theory. Zero-point-inclusive thermochemical corrections to energy were not included in each single point energy calculation, but were added to the subsequent activated complex, reactant and product energies for the activation barrier predictions. The calculated square of total spin is quite

close to its eigenvalues s (s + 1), indicating that the spin contamination is minor. For each of the open-shell species, H, HgBr, and Br, the deviation from $\langle s^2 \rangle$ is zero, 0.0081, and 0.00036, respectively.

The electronic transition from the $s^2$ ground state to the first excited state, $s^1p^1$ was calculated as 5.11 eV at the B3LYP/RCEP60VDZ level of theory. The available thermal energy at the maximum conditions considered, i.e., 2000K, is 0.172 eV, which is clearly not sufficient to produce this first excited state. Therefore, the $s^2$ ground state of $Hg^0$ was considered in all of the calculations.

The forward rate expressions are depicted graphically in Figures 4 and 5. The natural log of the rate constant as a function of inverse temperature is graphed along with error bars for each kinetic prediction. The details of each oxidation channel are discussed individually.

### *6.1.2 Mercury Oxidation via Bromine Radical*

A potential energy surface for reaction (1) is shown in Figure 1. This unimolecular recombination reaction is barrierless in the forward direction; therefore, variational RRKM was used to calculate the kinetic rate parameters. The values used for σ and ε/k were 4.0 Å and 400K, respectively, which were rough estimations; these numbers are typical for mercury-sized molecules in a bath gas.[62] By evaluating the associated trendlines over the given temperature range, the Arrhenius expressions are:

$$k_f^{RRKM} = 2.75 \times 10^{11} \exp\left(\frac{1.62}{RT}\right) \quad \left(\frac{cm^3}{mol \cdot s}\right) \qquad (9)$$

$$k_r^{RRKM} = 3.82 \times 10^{10} \exp\left(-\frac{14.1}{RT}\right) \quad \left(\frac{cm^3}{mol \cdot s}\right) \qquad (10)$$

The natural log of the forward rate constant ($cm^3$/molec/s) as a function of the inverse of temperature (K) is plotted in Figure 4 and compared with previously obtained theoretical and experimental values.

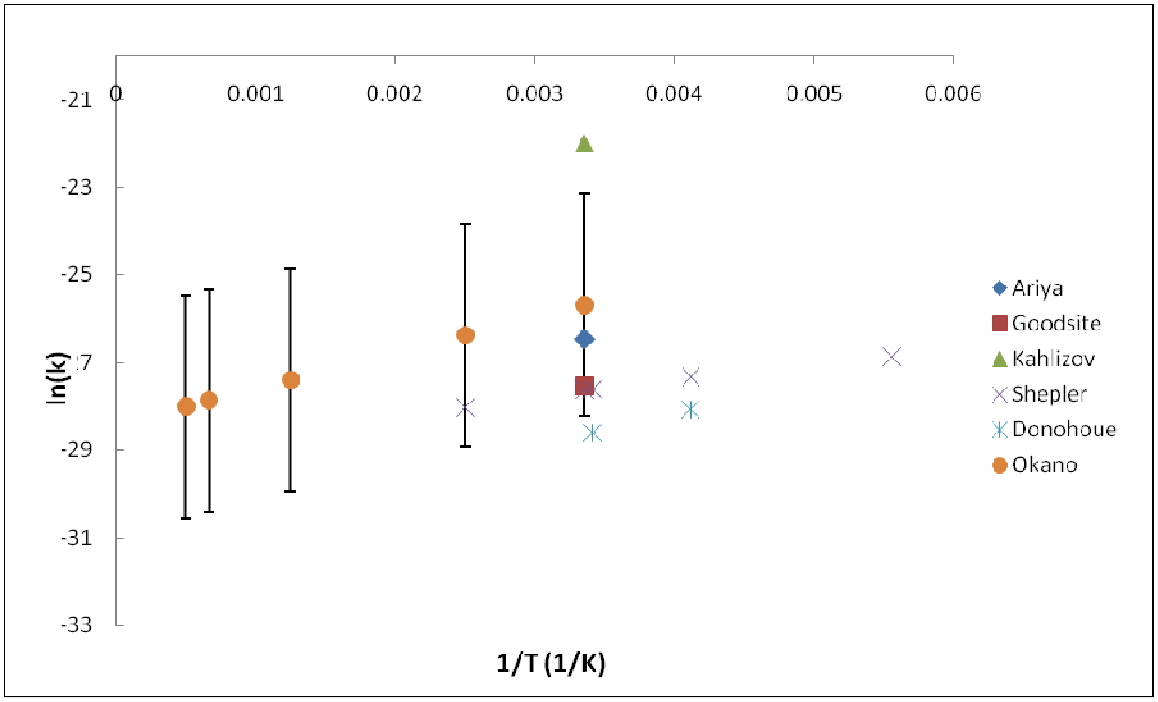


**Figure 4**. A comparison of reaction (1) rates with previous experimental (Ariya, Donohoue) and theoretical values (Goodsite, Khalizov, and Shepler). The error bars wholly encompass all of the data except for Donohoue's rates. Khalizov's rate constant is calculated at the high pressure limit and is shown to demonstrate the values calculated in this paper are well below this value.

An in-depth comparison of all the previous HgBr recombination reaction rates are given in Shepler[16], so this will not be repeated in the current work. The new data generated are expressed by the circles in Figure 4 with associated error bars. The largest source of error arises from the uncertainty of the activation energy due to the barrierless nature of the reaction. The reaction kinetics are chosen at the reaction coordinate where the rate starts to

level off or where there is minimal deviation. However, it is difficult to determine the exact point where this occurs. Other error can be accounted for by considering the lack of including correction for spin-orbit coupling, lamb shift, core valence energy,[16] and other such factors attributed to the difficulty in modeling large molecules. The error bars were generated based on the average reaction enthalpy deviations (1.6 kcal/mol) of the three reactions plus the magnitude of the spin orbit contribution for HgBr (0.8 kcal/mol).[31]

These correction factors were not included in our calculations because they proved to be insignificant for the current work. The goal was to obtain an accurate overall picture of the rates relative to each other and to show the validity of our reaction kinetics calculation methods. With the exception of Khalizov[30] and Donohoue[29], all of the other data points fall within the margin of error of the current predictions. The data point from Khalizov[30] is at the high pressure limit and was shown to demonstrate that our rate falls well below this value. Donohoue estimates an uncertainty of 50% for their rate constant, which overlaps with error margin of the current work. The general trend can be seen as a decrease in reaction rate with an increase in temperature, which is expected for a recombination reaction.

### *6.1.3 Mercury Oxidation via Bromine Gas*

The potential energy surface is plotted in Figure 2 and the saddle point is depicted on the surface at approximately (3.58 Å, 2.68 Å). The two variables examined in the linear transition structure were the Hg-Br and Br-Br bond distances. The transition structure parameters for the reaction are available in Table 5.

**Table 5**. Transition Structure Parameters for Reactions (2) and (3).

| | HgBrBr | HgBrH |
|---|---|---|
| bond length (Å) Hg-Br | 2.68 | 2.72 |
| bond length (Å) Br-Br; Br-H | 3.58 | 2.61 |
| bond angle (deg) | 180 | 180 |
| vibrational frequencies ($cm^{-1}$) | 20.64 | 137.61 |
| | 26.33 | 481.21 |
| | 131.88 | 481.21 |
| | 56.05*i* | 672.59*i* |
| single point energy (hartrees) | -5302.06 | -2728.45 |
| spin multiplicity | 3 | 1 |
| rotational constant (GHZ) | 0.222 | 1.15 |
| $I_{xx}$ (amu·Å$^2$) | 0 | 0 |
| $I_{yy}$ (amu·Å$^2$) | 2289.26 | 1747.32 |
| $I_{zz}$ (amu·Å$^2$) | 2289.26 | 1747.32 |

Evaluating the trendlines associated with each method shows that, over the given temperature range, the Arrhenius expressions are:

$$k_f^{TST} = 1.15 \times 10^{15} \exp\left(\frac{-30.1}{RT}\right) \left(\frac{cm^3}{mol \cdot s}\right) \qquad (13)$$

$$k_r^{TST} = 6.66 \times 10^{13} \exp\left(\frac{-2.3}{RT}\right) \left(\frac{cm^3}{mol \cdot s}\right) \qquad (14)$$

The natural log of the forward rate constant ($cm^3$/molec/s) as a function of the inverse of temperature (K) is plotted in Figure 5.

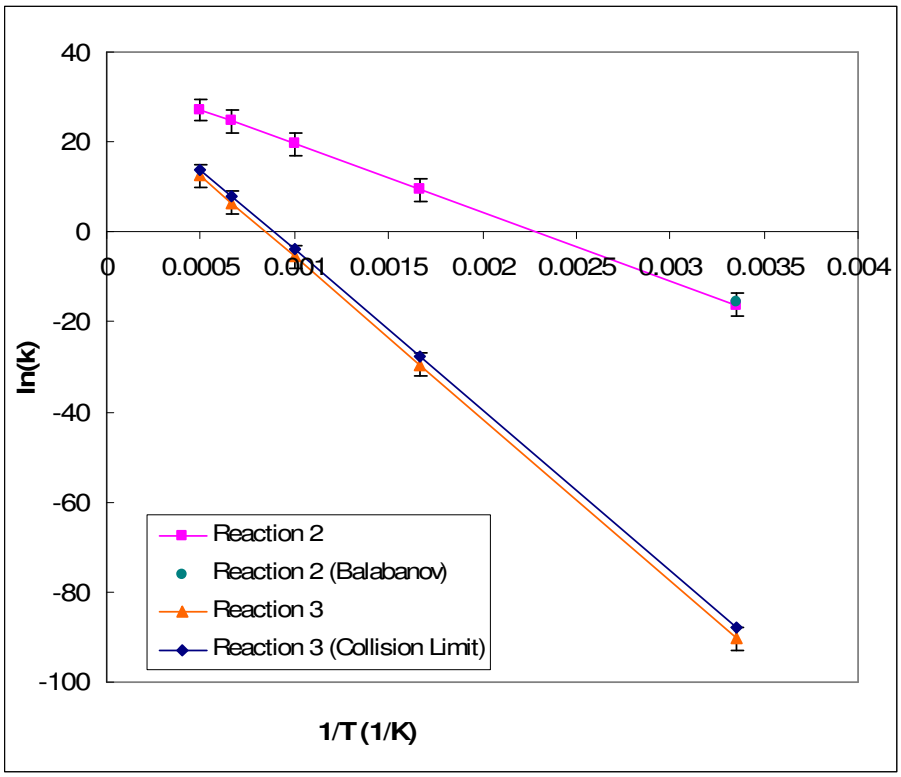


**Figure 5.** The natural log of the rate constants for reactions (2) and (3) as a function of inverse temperature. Also shown is a theoretical rate constant of reaction (2) by Balabanov and reaction (3) at the collision limit.

Comparison of these TST-derived rate constants can be made with the previous calculations carried out by Balabanov[32]. This author has a forward rate constant value of $3.4(\pm 0.15)\times 10^{-31}$ $cm^3$/molec/s at 298K which is about two times faster than the rate constant expressed in equation (13) ($1.60\times 10^{-31}$ $cm^3$/molec/s) at the same temperature. Balabanov's rate constant falls nicely within the error bar for the rate of reaction (2) at 298 K and proves the validity of the current method.

### *6.1.4 Mercury Oxidation via HBr*

The potential energy surface is similar to that of reaction (2) in that the saddle point can be visualized along the minimum energy path on the surface in Figure 3. A linear transition

structure was assumed for the triatomic activated complex, H-Br-Hg. An H-Br and Br-Hg distance of equal value, 2.73 Å, was found to possess at least one imaginary frequency indicative of a transition structure with the relevant parameters of the structure given in Table 2. Having identified the transition structure for this reaction, the kinetic rate parameters were then investigated using traditional TST. The natural log of the forward rate constant ($cm^3$/molec/s) as a function of the inverse of temperature (K) is plotted in Figure 5. The Arrhenius expressions were then determined to be:

$$k_f^{TST} = 1.86\times10^{13} \exp\left(-\frac{71.58}{RT}\right) \left(\frac{cm^3}{mol\cdot s}\right) \qquad (11)$$

$$k_r^{TST} = 3.65\times10^{12} \exp\left(-\frac{4.92}{RT}\right) \left(\frac{cm^3}{mol\cdot s}\right) \qquad (12)$$

A comparison of the TST activation energies to exact values calculated at each temperature shows that the forward reaction value of 71.58 kcal/mol deviated by at most 2.5 kcal/mol at 298 K, while the reverse reaction value of 4.92 kcal/mol deviated by at most 0.65 kcal/mol, reaching the maximum deviation at 2000 K. The forward reaction rate was compared to that calculated with simple collision theory to demonstrate that the rates are, although close, definitely below the collision limit.

## *6.2 Second-Stage Mercury Oxidation Reactions*

### *6.2.1 Potential Energy Surfaces*

Potential energy curves and surfaces generated for reactions (4) through (6) are shown in Figure 6 through 8, respectively.

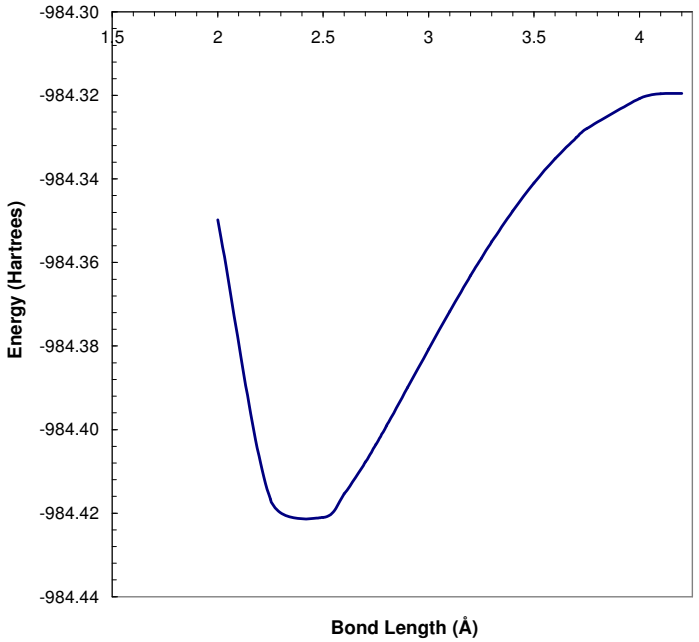


**Figure 6**. Reaction (4), $HgBr_2$ recombination, potential energy curve at CCSD(T)/AVTZ level of theory.

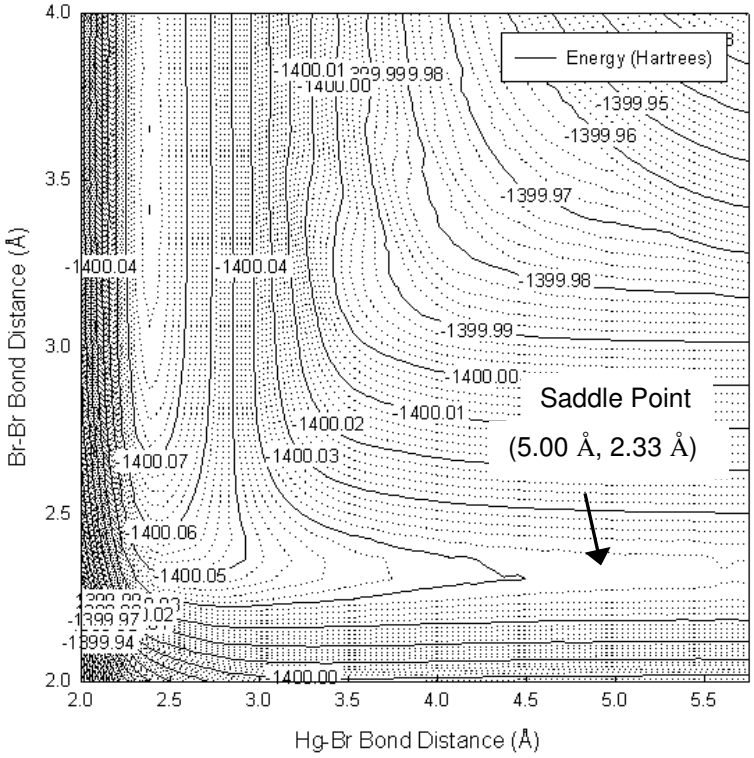


**Figure 7**. Reaction (5), HgBr + $Br_2$ → $HgBr_2$ + Br, potential energy surface at CCSD(T)/AVTZ level of theory. It is a barrierless reaction in the forward direction.

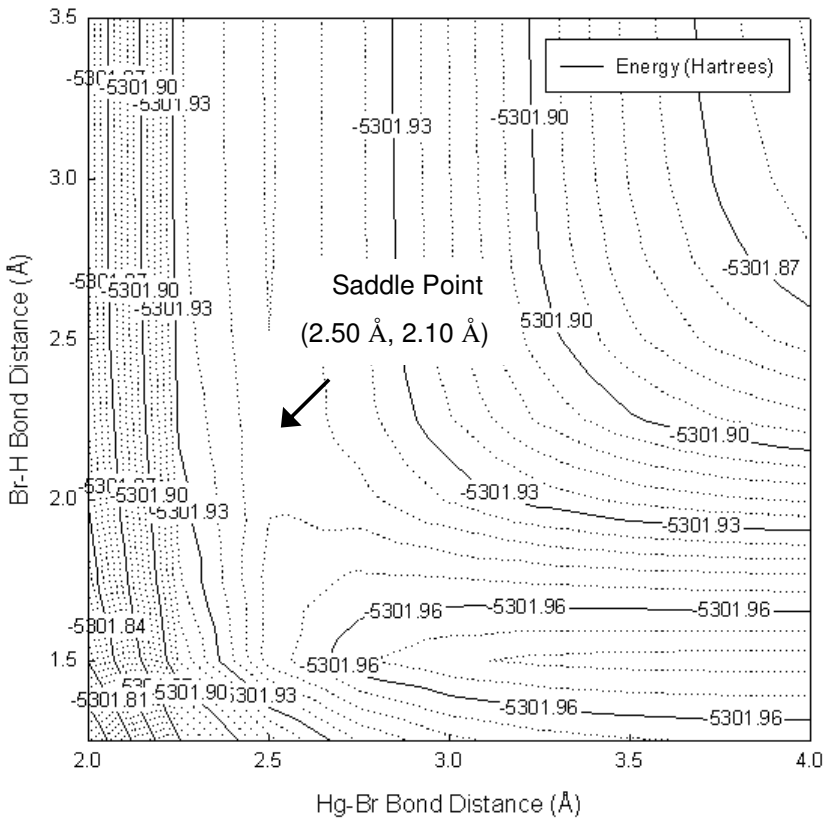


**Figure 8**. Reaction (6), HgBr + HBr → $HgBr_2$ + H, potential energy surface at B3LYP/ECP60MDF level of theory. The remaining Hg-Br bond was assumed to be constant at 2.54 Å.

The HgBr + Br recombination potential energy curve was produced at the CCSD(T)/AVTZ level of theory. It is a typical curve with the potential well representing the equilibrium energy between HgBr and Br, i.e., the $HgBr_2$ molecule. Unrestricted CCSD(T) was employed for all open-shell systems, which included all the single point energy calculations for the reactants in reaction (4). The two contour surfaces for reactions (5) and (6) were generated with approximately 200 single-point energy calculations at the CCSD(T)/AVTZ and B3LYP/ECP60MDF level of theory, respectively. Similar to the first set of reactions, zero-point-inclusive thermochemical corrections to energy were not included

in each single point energy calculation, but were added to the subsequent activated complex, reactant and product energies for the activation barrier predictions.

The forward rate expressions are depicted graphically in Figure 9 and 10. The natural log of the rate constant as a function of inverse temperature is graphed along with error bars for each kinetic prediction. The details of each oxidation channel are discussed individually.

### *6.2.2 Mercury-Bromine Radical Recombination with Bromine Radical*

A potential energy surface for reaction (4) is shown in Figure 6. This unimolecular recombination reaction is barrierless in the forward direction; therefore, variational RRKM was used to calculate the kinetic rate parameters. A value of 4.0 Å for σ and 500K for ε/k were estimated from available critical properties.[63,64] The natural log of the forward rate constant ($cm^3$/molec/s) as a function of the inverse of temperature (K) is plotted in Figure 9 and compared with previously obtained theoretical values.

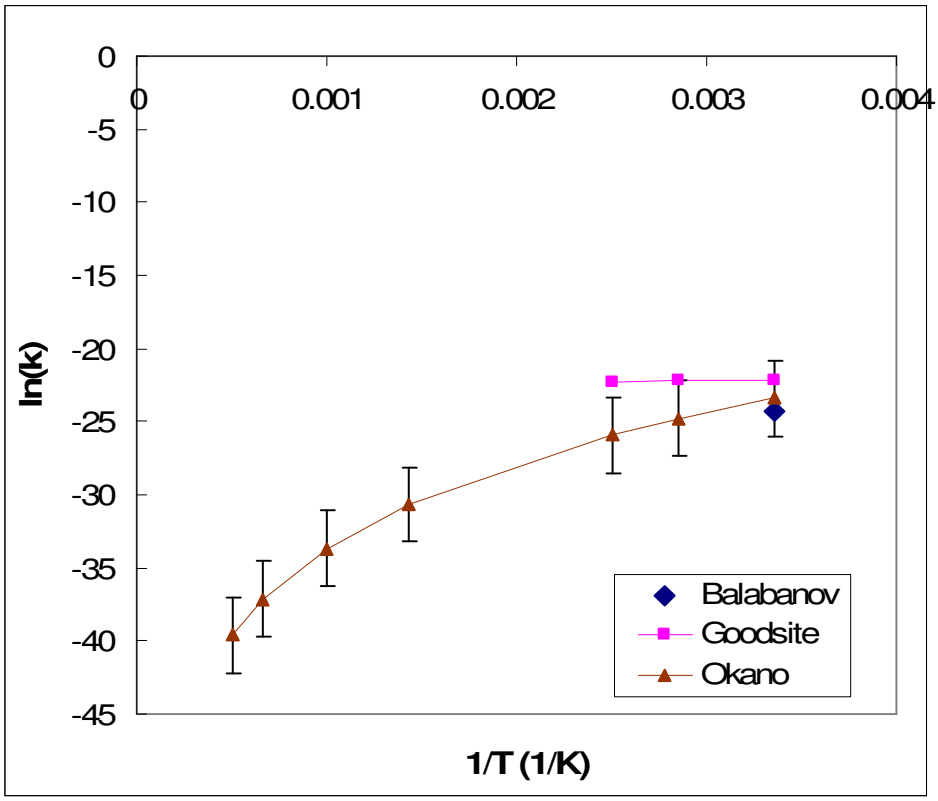


**Figure 9.** A comparison of reaction (4) rate constants shows an overall negative temperature dependence, as expected, for a unimolecular decomposition reaction. The calculated value at 298 K falls directly between those of Balabanov and Goodsite.

By evaluating the associated trendlines over the given temperature range, the Arrhenius expressions are:

$$k_f^{RRKM} = 4.11\times10^{13}\left(\frac{T}{298K}\right)^{-8.5}\quad\left(\frac{cm^3}{mol\cdot s}\right) \qquad (13)$$

$$k_r^{RRKM} = 2.73\times10^{7}\exp\left(-\frac{58.2}{RT}\right)\quad\left(\frac{1}{s}\right) \qquad (14)$$

A comparison of these values to those of Goodsite[31] and Balabanov[32] proves there is a very good correlation between all three data sets; the calculated rate constant falls directly between the two values. As can be seen in Figure 4, Balabanov's rate constant is slightly

slower and Goodsite's rate is five times faster. Goodsite has a rate expression with a temperature range of 180-400 K that has a slightly negative temperature dependence. Our calculated values have a highly negative temperature dependence, as expected, which can be explained from a thermodynamic point of view. At 298 K, the Gibbs free energy of the reaction is -64 kcal/mol, whereas at 2000 K, it is +10 kcal/mol. This change in sign indicates a dramatic preference for the reaction to proceed in the forward direction at lower temperatures, but the opposite at very high temperatures. Because of this, the reaction rates are highly sensitive to the temperature at which the reaction takes place.

As was the case for reaction (1), the largest source of error arises from the uncertainty of the activation energy due to the barrierless nature of the reaction. Other error can be accounted for by considering the lack of including correction factors. Since the reaction enthalpy values were accurate within 1 kcal/mol for reactions (4) – (6), the error bars were generated conservatively based on the error obtained from reactions (1)-(3).

### *6.2.3 Mercury-Bromine Radical Oxidation via Bromine Gas*

The potential energy surface is plotted at the CCSD(T)/AVTZ level of theory in Figure 7 and the saddle point can be visualized along the reaction path at approximately (5.00 Å, 2.33 Å). The two variables examined in the linear transition structure were the bond distances for the forming Hg-Br bond and the breaking Br-Br bond; for simplicity, the one bond that does not form or break (Br-Hg) was kept constant and estimated to be 2.47 Å, the average distance between the HgBr and $HgBr_2$ molecule at the CCSD(T)/AVTZ level of theory. The transition

state parameters for the reaction were obtained from the potential energy surface and are available in Table 6.

**Table 6.** Transition structure parameters for reactions (5) and (6).

| | **BrHgBrBr** | **BrHgBrH** |
|---|---|---|
| bond length (Å) (Br-Hg)-Br-X | 2.47 | 2.54 |
| bond length (Å) Br-(Hg-Br)-X | 5.70 | 2.50 |
| bond length (Å) Br-Hg-(Br-X) | 2.33 | 2.10 |
| bond angle (deg) | 180 | 180 |
| vibrational frequencies ($cm^{-1}$) | 303.01 | 51.59 |
| | 213 | 51.59 |
| | 27.69 | 76.53 |
| | 27.69 | 76.53 |
| | 2.83 | 194.78 |
| | 30.27*i* | 255.12 |
| | 30.27*i* | 471.12*i* |
| single point energy (hartrees) | -1400.03 | -5301.95 |
| spin multiplicity | 2 | 2 |
| rotational constant (GHZ) | 0.094 | 0.493 |
| $I_{xx}$ (amu·Å$^2$) | 0 | 0 |
| $I_{yy}$ (amu·Å$^2$) | 5756 | 1036 |
| $I_{zz}$ (amu·Å$^2$) | 5756 | 1036 |

The natural log of the forward rate constant ($cm^3$/molec/s) as a function of the inverse of temperature (K) is plotted in Figure 10. There are two imaginary frequencies for reaction (5) in the first column in Table 6. This is mostly likely because of the assumption of a linear transition state. It is indicative of a local minimum that is in the vicinity of the transition state. Due to lack of time and resources, a reaction rate was determined with these frequencies. It will be necessary to recalculate the transition state with more accuracy.

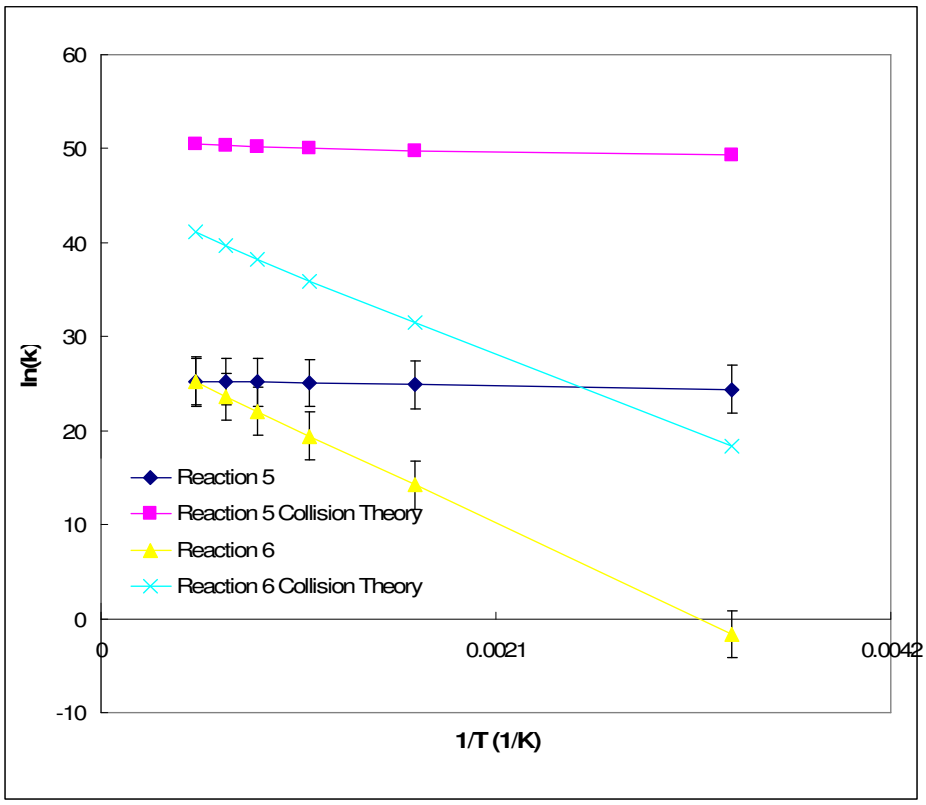


**Figure 10.** The natural log of the rates for reactions (5) and (6) and corresponding rates calculated by collision theory, which determines the upper limit. Both reactions are well below their collision limits.

Reaction (5) has only slight temperature dependence. This is a result of it being a barrierless reaction in the forward direction. The increased energy through stronger collisions at the higher temperatures has little effect on the reaction. Evaluating the trendlines over the given temperature range, the Arrhenius expressions are:

$$k_f^{TST} = 4.06\times10^{11} \exp\left(\frac{-0.87}{RT}\right)\left(\frac{cm^3}{mol\cdot s}\right) \qquad (15)$$

$$k_r^{TST} = 4.30\times10^{12} \exp\left(\frac{-24.5}{RT}\right)\left(\frac{cm^3}{mol\cdot s}\right) \qquad (16)$$

Since there is not a way to compare these numbers to previous calculations or experiment, Figure 5 shows the upper bound from collision theory calculations. The reaction rates fall well below the collision theory numbers indicating they are within reason.

### *6.2.4 Mercury-Bromine Radical Oxidation via HBr*

The potential energy surface for reaction (6) created at the B3LYP/ECP60MDF level of theory has a saddle point at (2.50 Å, 2.10 Å), along the reaction path. A linear transition structure was assumed for the quadratomic activated complex, H-Br-Hg-Br. The Hg-Br bond which was not forming or breaking was kept constant at distance of 2.54 Å, the average of the bond distances of the HgBr and $HgBr_2$ molecule at the same level of theory. Relevant transition structure parameters are given in Table 6. Having identified the transition structure for this reaction, the kinetic rate parameters were then investigated using traditional TST. The natural log of the forward rate constant ($cm^3$/molec/s) as a function of the inverse of temperature (K) is plotted in Figure 10. The Arrhenius expressions were then determined to be:

$$k_f^{TST} = 9.41\times10^{12}\exp\left(-\frac{18.6}{RT}\right)\ \left(\frac{cm^3}{mol\cdot s}\right) \qquad (17)$$

$$k_r^{TST} = 1.17\times10^{15}\exp\left(-\frac{3.58}{RT}\right)\ \left(\frac{cm^3}{mol\cdot s}\right) \qquad (18)$$

A comparison of the TST activation energies to exact values calculated at each temperature shows that the forward reaction value of 18.6 kcal/mol deviated by at most 4.7 kcal/mol at 2000 K while the reverse reaction value of 3.58 kcal/mol deviated by at most 1.4 kcal/mol, reaching the maximum deviation at 298.15 K. Similar to reaction (2), as there was

no data to compare to reaction (3), the rate constants were compared to those calculated by collision theory and were found to fall desirably below the upper limit.

## Chapter 7: Conclusions

Accurate *ab inito* reaction kinetics data for six mercury-bromine oxidation reactions were calculated. First, the appropriate level of theory was determined from the accuracy of the reaction enthalpies and then a potential energy surface was constructed. Depending on the type of reaction, bimolecular or unimolecular, TST or RRKM was used, respectively, to calculate the reaction kinetics.

Of the six reactions, only one had experimental values available in the literature and only three reactions had theoretical values with which to compare to the current data. Of the rate constants that had comparisons available, nearly all previously calculated kinetics fell within the error margins. The calculations of these rate constants allows this work to move one step ahead to now compare the kinetics and elucidate the most dominant pathways for mercury-bromine oxidation.

These reactions, combined with the following hydrogen bromine kinetics:

$$Br_2 + M \rightarrow 2Br + M \quad (19)$$

$$H_2 + M \rightarrow 2H + M \quad (20)$$

$$H_2 + Br \rightarrow H + HBr \quad (21)$$

$$H + Br_2 \rightarrow HBr + Br \quad (22)$$

$$HBr + M \rightarrow H + Br + M \quad (23)$$

will be studied using reaction route graph theory[65] to find the path of least resistance and to ultimately establish a mercury-bromine submechanism. The creation of such a submechanism to add to an existing global combustion mechanism will greatly enhance the ability to predict mercury speciation in coal combustion flue gases containing bromine.

# Appendix A

## A.1 Gaussian Inputs

**Example 1**: Input file for calculating a single point energy with a given geometry and obtain frequencies and thermodynamics; HgCl2 at PW91/Aug-cc-pVTZ level of theory

Filename: 6M1HgCl2.gjf

```
%chk=6M1HgCl2.chk
#PW91PW91/gen pseudo=read freq=numer

HgCl2 opt freq

0 1
Hg
Cl 1 R1
Cl 2 R2 1 A1

R1 2.36
R2 3.00
A1 179.999

HG     0
S     9     1.00
             98.3058000              0.0010330
             19.6406000             -0.1063820
             12.3397000              0.5320730
              7.7478200             -0.5223240
              4.8629100             -0.5373210
              1.5771900              0.8847880
              0.7529260              0.5138340
              0.2351120              0.0294070
              0.1039680             -0.0061590
S     9     1.00
             98.3058000             -0.0003560
             19.6406000              0.0379090
             12.3397000             -0.2000130
              7.7478200              0.2240930
              4.8629100              0.1793740
              1.5771900             -0.4508330
              0.7529260             -0.3390550
              0.2351120              0.2934140
              0.1039680              0.6446280
S     9     1.00
             98.3058000             -0.0002170
             19.6406000             -0.0440670
             12.3397000              0.2876950
              7.7478200             -0.1894760
              4.8629100             -0.7807040
              1.5771900              2.1756040
              0.7529260             -0.8865840
              0.2351120             -1.8749170
```

```
                0.1039680             1.2470530
S       9       1.00
                98.3058000           -0.0020930
                19.6406000            0.1557830
                12.3397000           -0.7951410
                 7.7478200            0.9970540
                 4.8629100            0.5928610
                 1.5771900           -4.4071970
                 0.7529260            5.2898370
                 0.2351120           -2.8866330
                 0.1039680            0.3158740
S       1       1.00
                 0.0434000            1.0000000
P       8       1.00
                21.4065000           -0.0128370
                13.3929000            0.0865310
                 6.5102100           -0.3080410
                 1.8222200            0.5327940
                 0.9265070            0.4822070
                 0.4550820            0.1546950
                 0.1927600            0.0132010
                 0.0786890            0.0005850
P       8       1.00
                21.4065000            0.0026690
                13.3929000           -0.0218770
                 6.5102100            0.0865390
                 1.8222200           -0.1847680
                 0.9265070           -0.1773950
                 0.4550820            0.0009770
                 0.1927600            0.3536030
                 0.0786890            0.5435820
P       8       1.00
                21.4065000            0.0061400
                13.3929000           -0.0480560
                 6.5102100            0.1891060
                 1.8222200           -0.4381190
                 0.9265070           -0.4321930
                 0.4550820            0.4570570
                 0.1927600            0.6953570
                 0.0786890            0.1420160
P       8       1.00
                21.4065000            0.0130140
                13.3929000           -0.0890970
                 6.5102100            0.3480200
                 1.8222200           -1.2184470
                 0.9265070            0.1232280
                 0.4550820            1.6284380
                 0.1927600           -0.7824510
                 0.0786890           -0.5112540
P       1       1.00
                 0.0317290            1.0000000
D       7       1.00
                86.9881000            0.0000580
                11.9913000            0.0127790
                 6.9364800           -0.0689630
```

```
              2.0864100             0.2415630
              1.0766400             0.3878580
              0.5311530             0.3454410
              0.2488080             0.1915090
D     7     1.00
             86.9881000             0.0000500
             11.9913000             0.0192460
              6.9364800            -0.1034870
              2.0864100             0.4847690
              1.0766400             0.5069510
              0.5311530            -0.3625720
              0.2488080            -0.5729800
D     7     1.00
             86.9881000            -0.0000430
             11.9913000             0.0337600
              6.9364800            -0.1746100
              2.0864100             1.2017020
              1.0766400            -0.5030930
              0.5311530            -1.1299990
              0.2488080             0.7749310
D     1     1.00
              0.1081700             1.0000000
F     1     1.00
              1.5814000             1.0000000
F     1     1.00
              0.5423000             1.0000000
G     1     1.00
              1.3737000             1.0000000
S     1     1.00
              0.0181000             1.0000000
P     1     1.00
              0.0128000             1.0000000
D     1     1.00
              0.0470000             1.0000000
F     1     1.00
              0.2182000             1.0000000
G     1     1.00
              0.6361000             1.0000000
****
CL     0
S     13     1.00
         456100.0000000             0.492970D-04
          68330.0000000             0.383029D-03
          15550.0000000             0.200854D-02
           4405.0000000             0.838558D-02
           1439.0000000             0.294703D-01
            520.4000000             0.878325D-01
            203.1000000             0.211473D+00
             83.9600000             0.365364D+00
             36.2000000             0.340884D+00
             15.8300000             0.102133D+00
              6.3340000             0.311675D-02
              2.6940000             0.105751D-02
              0.4313000             0.156136D-03
S     13     1.00
```

```
          456100.0000000             -0.138304D-04
           68330.0000000             -0.107279D-03
           15550.0000000             -0.565083D-03
            4405.0000000             -0.236135D-02
            1439.0000000             -0.845886D-02
             520.4000000             -0.259638D-01
             203.1000000             -0.686362D-01
              83.9600000             -0.141874D+00
              36.2000000             -0.199319D+00
              15.8300000             -0.195662D-01
               6.3340000              0.499741D+00
               2.6940000              0.563736D+00
               0.4313000             -0.835091D-02
S     13     1.00
          456100.0000000              0.418546D-05
           68330.0000000              0.324395D-04
           15550.0000000              0.171105D-03
            4405.0000000              0.714176D-03
            1439.0000000              0.256705D-02
             520.4000000              0.788552D-02
             203.1000000              0.210867D-01
              83.9600000              0.442264D-01
              36.2000000              0.651670D-01
              15.8300000              0.603012D-02
               6.3340000             -0.206495D+00
               2.6940000             -0.405871D+00
               0.4313000              0.725661D+00
S     1      1.00
               0.9768000              1.0000000
S     1      1.00
               0.1625000              1.0000000
P     7      1.00
             663.3000000              0.240448D-02
             156.8000000              0.192148D-01
              49.9800000              0.885097D-01
              18.4200000              0.256020D+00
               7.2400000              0.436927D+00
               2.9220000              0.350334D+00
               0.3818000             -0.458423D-02
P     7      1.00
             663.3000000             -0.652145D-03
             156.8000000             -0.519445D-02
              49.9800000             -0.246938D-01
              18.4200000             -0.728167D-01
               7.2400000             -0.134030D+00
               2.9220000             -0.947742D-01
               0.3818000              0.564667D+00
P     1      1.00
               1.0220000              1.0000000
P     1      1.00
               0.1301000              1.0000000
D     1      1.00
               1.0460000              1.0000000
D     1      1.00
               0.3440000              1.0000000
```

```
F     1     1.00
              0.7060000             1.0000000
S     1     1.00
              0.0591000             1.0000000
P     1     1.00
              0.0419000             1.0000000
D     1     1.00
              0.1350000             1.0000000
F     1     1.00
              0.3120000             1.0000000
****

HG     0
HG-ECP   5   60
H POTENTIAL
  1
2               1.0000000              0.0000000
S-H POTENTIAL
  2
2              12.4130710            275.7747970
2               6.8979130             49.2678980
P-H POTENTIAL
  4
2              11.3103200             80.5069840
2              10.2107730            161.0348240
2               5.9398040              9.0834160
2               5.0197550             18.3677730
D-H POTENTIAL
  4
2               8.4078950             51.1372560
2               8.2140860             76.7074590
2               4.0126120              6.5618210
2               3.7953980              9.8180700
F-H POTENTIAL
  2
2               3.2731060              9.4290010
2               3.2083210             12.4948560
G-H POTENTIAL
  2
2               4.4852960             -6.3384140
2               4.5132000             -8.0998630
```

---

**Example 2**: Input file for finding the optimized (lowest energy state) geometry for a molecule and obtain frequencies and thermodynamics; HgBr2 at B3LYP/Aug-cc-pVTZ level of theory.

Filename: HgBr2B3LYPAugpVTZ.gjf

---

```
%chk=HgBr2B3LYPAugpVTZ.chk
#B3LYP/gen pseudo=read opt freq=numer
```

```
HgBr2 opt freq no pp on Br

0 1
Br
Hg 1 R1
Br 2 R1 1 A1

R1 2.42
A1 179.999

BR     0
S     7     1.00
           9659.3900000             0.0003710
           1455.9600000             0.0025710
            325.9140000             0.0084850
             46.5657000             0.0782220
             18.2469000            -0.3971490
              3.8020100             0.6858640
              1.7863200             0.4868190
S     7     1.00
           9659.3900000            -0.0001520
           1455.9600000            -0.0010080
            325.9140000            -0.0036090
             46.5657000            -0.0278720
             18.2469000             0.1513170
              3.8020100            -0.3514970
              1.7863200            -0.4107030
S     1     1.00
              0.6027140             1.0000000
S     1     1.00
              0.2840140             1.0000000
S     1     1.00
              0.1202710             1.0000000
P     9     1.00
            492.1870000             0.0004720
             92.3642000             0.0054940
             27.0718000            -0.0880300
              7.2653900             0.3434850
              3.4848100             0.5102080
              1.6404800             0.2486310
              0.6485700             0.0222010
              0.2564070            -0.0004190
              0.0953040             0.0006560
P     9     1.00
            492.1870000            -0.0001580
             92.3642000            -0.0013440
             27.0718000             0.0246160
              7.2653900            -0.1125320
              3.4848100            -0.1797750
              1.6404800            -0.0736610
              0.6485700             0.3487340
              0.2564070             0.5579480
              0.0953040             0.2664560
P     1     1.00
              0.7666000             1.0000000
```

```
P      1     1.00
              0.1182000             1.0000000
D      7     1.00
            338.9960000             0.0015240
            103.2170000             0.0156730
             42.3638000             0.0724000
             18.4356000             0.1863030
              8.3725400             0.3238810
              3.8022200             0.3745340
              1.6867700             0.2574180
D      1     1.00
              0.6775200             1.0000000
D      1     1.00
              0.2553000             1.0000000
F      1     1.00
              0.5606000             1.0000000
S      1     1.00
              0.0445000             1.0000000
P      1     1.00
              0.0396000             1.0000000
D      1     1.00
              0.1009000             1.0000000
F      1     1.00
              0.2454000             1.0000000
****
HG     0
S      9     1.00
             98.3058000             0.0010330
             19.6406000            -0.1063820
             12.3397000             0.5320730
              7.7478200            -0.5223240
              4.8629100            -0.5373210
              1.5771900             0.8847880
              0.7529260             0.5138340
              0.2351120             0.0294070
              0.1039680            -0.0061590
S      9     1.00
             98.3058000            -0.0003560
             19.6406000             0.0379090
             12.3397000            -0.2000130
              7.7478200             0.2240930
              4.8629100             0.1793740
              1.5771900            -0.4508330
              0.7529260            -0.3390550
              0.2351120             0.2934140
              0.1039680             0.6446280
S      9     1.00
             98.3058000            -0.0002170
             19.6406000            -0.0440670
             12.3397000             0.2876950
              7.7478200            -0.1894760
              4.8629100            -0.7807040
              1.5771900             2.1756040
              0.7529260            -0.8865840
              0.2351120            -1.8749170
```

```
                0.1039680             1.2470530
S     9     1.00
              98.3058000            -0.0020930
              19.6406000             0.1557830
              12.3397000            -0.7951410
               7.7478200             0.9970540
               4.8629100             0.5928610
               1.5771900            -4.4071970
               0.7529260             5.2898370
               0.2351120            -2.8866330
               0.1039680             0.3158740
S     1     1.00
               0.0434000             1.0000000
P     8     1.00
              21.4065000            -0.0128370
              13.3929000             0.0865310
               6.5102100            -0.3080410
               1.8222200             0.5327940
               0.9265070             0.4822070
               0.4550820             0.1546950
               0.1927600             0.0132010
               0.0786890             0.0005850
P     8     1.00
              21.4065000             0.0026690
              13.3929000            -0.0218770
               6.5102100             0.0865390
               1.8222200            -0.1847680
               0.9265070            -0.1773950
               0.4550820             0.0009770
               0.1927600             0.3536030
               0.0786890             0.5435820
P     8     1.00
              21.4065000             0.0061400
              13.3929000            -0.0480560
               6.5102100             0.1891060
               1.8222200            -0.4381190
               0.9265070            -0.4321930
               0.4550820             0.4570570
               0.1927600             0.6953570
               0.0786890             0.1420160
P     8     1.00
              21.4065000             0.0130140
              13.3929000            -0.0890970
               6.5102100             0.3480200
               1.8222200            -1.2184470
               0.9265070             0.1232280
               0.4550820             1.6284380
               0.1927600            -0.7824510
               0.0786890            -0.5112540
P     1     1.00
               0.0317290             1.0000000
D     7     1.00
              86.9881000             0.0000580
              11.9913000             0.0127790
               6.9364800            -0.0689630
```

```
              2.0864100             0.2415630
              1.0766400             0.3878580
              0.5311530             0.3454410
              0.2488080             0.1915090
D     7     1.00
             86.9881000             0.0000500
             11.9913000             0.0192460
              6.9364800            -0.1034870
              2.0864100             0.4847690
              1.0766400             0.5069510
              0.5311530            -0.3625720
              0.2488080            -0.5729800
D     7     1.00
             86.9881000            -0.0000430
             11.9913000             0.0337600
              6.9364800            -0.1746100
              2.0864100             1.2017020
              1.0766400            -0.5030930
              0.5311530            -1.1299990
              0.2488080             0.7749310
D     1     1.00
              0.1081700             1.0000000
F     1     1.00
              1.5814000             1.0000000
F     1     1.00
              0.5423000             1.0000000
G     1     1.00
              1.3737000             1.0000000
S     1     1.00
              0.0181000             1.0000000
P     1     1.00
              0.0128000             1.0000000
D     1     1.00
              0.0470000             1.0000000
F     1     1.00
              0.2182000             1.0000000
G     1     1.00
              0.6361000             1.0000000
****

BR     0
BR-ECP   4   10
G POTENTIAL
  1
2              1.0000000              0.0000000
S-G POTENTIAL
  3
2             70.0242570             49.9628340
2             31.1784120            370.0142050
2              7.1565930             10.2414390
P-G POTENTIAL
  4
2             46.7734710             99.1122440
2             46.1841200            198.2530460
2             21.7138580             28.2617400
```

```
2             20.9417920             56.6233660
D-G POTENTIAL
  6
2             50.6988390            -18.6058530
2             50.6447640            -27.9232800
2             15.4475090             -0.3796930
2             15.5002590             -0.7805830
2              2.8003910              0.0359680
2              1.0774800              0.0943970
F-G POTENTIAL
  2
2             14.4656060             -1.0912690
2             21.2340650             -2.8876910
HG     0
HG-ECP   5   60
H POTENTIAL
  1
2              1.0000000              0.0000000
S-H POTENTIAL
  2
2             12.4130710            275.7747970
2              6.8979130             49.2678980
P-H POTENTIAL
  4
2             11.3103200             80.5069840
2             10.2107730            161.0348240
2              5.9398040              9.0834160
2              5.0197550             18.3677730
D-H POTENTIAL
  4
2              8.4078950             51.1372560
2              8.2140860             76.7074590
2              4.0126120              6.5618210
2              3.7953980              9.8180700
F-H POTENTIAL
  2
2              3.2731060              9.4290010
2              3.2083210             12.4948560
G-H POTENTIAL
  2
2              4.4852960             -6.3384140
2              4.5132000             -8.0998630
```

---

**Example 3**: Directions for obtaining thermodynamics and partition functions at different temperatures

Freqchk Instructions:

1. Copy the freqchk.exe file (from myWPI under course documents) in your C: directory or a location that's accessible from your current computer.
2. Copy the checkpoint file from WebMO (or from the scratch folder in Gaussian) into this same location/folder.

2. Under 'start' and 'accessories', go to the 'command prompt,' and to the directory that you just placed the freqchk.exe file, e.g. C:\Documents and Settings...
3. Type 'freqchk,' and it will ask which file and then enter the filename (don't forget it's a .chk file).
4. It will ask a series of questions, e.g. temp (your desired temp), press (typically 1.0 atm), scale factor (1.0), isotopes (no), etc.
5. For each temperature you can generate the required frequency data.

### A.2 Gaussian Outputs from Examples 1-3

**Table A1.** Output values from Examples 1 & 2 needed for reaction kinetics calculation. (Energies are in hartrees/particle.)

| | $HgBr_2$ | $HgCl_2$ |
|---|---|---|
| **Level of Theory** | B3LYP/Aug-cc-pVTZ | PW91/Aug-cc-pVTZ |
| **Geometry (Å)** | 2.4247 (optimized) | 2.36 (given) |
| | 180.0˚ | 3.00 (given) |
| | -- | 179.999˚ |
| **Ground State Energy** | -987.4611542 | -1073.961616 |
| **Thermal Correction @ 298K** | 0.006363 | 0.005344 |
| **Frequenc(ies)** | 65.7155 | -105.7059 |
| | 65.7155 | 92.8200 |
| | 205.9729 | 92.8200 |
| | 274.2768 | 258.3512 |
| **Partition Coefficient (Q)** | | |
| **Electronic** | 1 | 1 |
| **Translational** | 2.68E+08 | 1.76E+08 |
| **Rotational** | 5.70E+03 | 1.14E+04 |

**Table A2.** Output values from Example 3 needed for reaction kinetics calculation.

| Temperature (K) | Thermal correction (Hartree/particle) | Partition Coefficients (Q) | | |
|---|---|---|---|---|
| | | Electronic | Translational | Rotational |
| 600 | 0.010527 | 1 | 1.01E+09 | 2.30E+04 |
| 900 | 0.015727 | 1 | 2.79E+09 | 3.46E+04 |
| 1200 | 0.020939 | 1 | 5.73E+09 | 4.61E+04 |
| 1500 | 0.026157 | 1 | 1.00E+10 | 5.76E+04 |
| 2000 | 0.034858 | 1 | 2.05E+10 | 7.68E+04 |

# Appendix B

## B.1 How to Run MOLPRO (remotely as a non-Stanford student)

**Access the computers with MOLPRO**

1. Obtain a SUNet ID from this website: http://sunetid.stanford.edu/.
2. Download the Stanford VPN client from: http://stanford.edu/services/vpn. The VPN is already configured for Stanford connections.
3. If using Windows, get SSH and FTP from: http://ess.stanford.edu (look for SecureCRT and SecureFX.)
4. MOLPRO is available on Sparc and Opteron clusters.
5. If you use SecureCRT or SecureFX from a Windows machine to connect to cees-sparc, you will need to make 'keyboard-interactive' the first authentication method SecureCRT or SecureFX tries. This can be found by right clicking the hostname in the session window and selecting properties, then clicking on SSH2. You will see the authentication window in the middle. Highlight 'keyboard-interactive' and move it to the first position. 6. Establish a connection with SecureCRT and SecureFX by clicking 'Connect' and then the name of the cluster you want to connect to, either cees-sparc.stanford.edu or cees-opteron.stanford.edu. Enter your username and password to login.

**Set up Computer Environment to Run MOLPRO**

1. Create the scratch directories. These will work on both clusters. (Substitute $USER with your username.)

Log onto cees-opteron or cees-sparc
% mkdir /data/temp1/$USER
% mkdir /data/temp1/$USER/MOLPROSCR
% mkdir /data/temp2/$USER
% mkdir /data/temp2/$USER/MOLPROSCR

2. Create the wfu directory on both clusters in your home directory, or just on the cluster of your choice. (Substitute $USER with your username.)

Log onto cees-opteron
% mkdir $HOME/wfu
Log onto cees-sparc
% mkdir $HOME/wfu

3. Create $HOME/Results directory on both cees-opteron and cees-sparc. ( Substitute $HOME with home/'your username'.)

% mkdir $HOME/Results

4. Put the following in your .tcshrc on the Opteron Cluster. This step is not necessary on the Sparc Cluster.

Log onto cees-opteron and edit the .tcshrc and add this at the bottom:

```
if ( -d /usr/local/molpro ) then
  setenv LD_PRELOAD /lib64/tls/libpthread.so.0
  setenv MOLPRO_KEY
"id-stan,date=:2008/07/17,version=:2006&ZL5C8gdnQLgDwYjL"
  setenv MOLPRO_SCR
"/data/temp1/$USER/MOLPROSCR:/data/temp2/$USER/MOLPROSCR"
  setenv LIMBOL "/usr/local/lib/Molpro"
endif
```

5. Edit these submit scripts for the name of the SGE results directory, the number of cpus, and the input filename. Note that the '-pe' line is different, and the Sparc doesn't need a '-q' line. These submit scripts can be found in Dennis' home directory - /home/dennis/molpro/testmol.sh.

Opteron Cluster:

```
#!/bin/tcsh
#$ -S /bin/tcsh
#$ -pe mpich8 2
#$ -q 8GB.q
#$ -e $HOME/Results
#$ -o $HOME/Results
#$ -cwd
#
molpro -n $NSLOTS --mpirun-machinefile $TMPDIR/machines INPUTFILENAME.inp
```

2. The amount of memory needed for the run can be set on the second line in the input file. If there is insufficient memory, usually the output file will tell you how much more is needed.

3. The commands: "file,1,xxx.int" and "file,2,xxx.wfu" should be used in the input file (right after the memory, if specified) when thermodynamics and partition functions will be needed at different temperatures.

Sparc Cluster:

```
#!/bin/tcsh
#$ -S /bin/tcsh
#$ -pe mpich 2
#$ -e $HOME/Results
#$ -o $HOME/Results
#$ -cwd
```

```
#
molpro -n $NSLOTS --mpirun-machinefile $TMPDIR/machines INPUTFILENAME.inp
```

6. Submit the scripts in the usual way:

```
% qsub testmol.sh
```

**B.2 Useful Tips for Running MOLPRO**

1. Input files are best created in Notepad. Change the file to an ".inp" file. Output files, ".out," are best viewed with Wordpad.
2. Basic commands:
   To edit an input file, type 'pico xxx.inp.'
   To check the queue, type 'qstat.' Jobs in state 'qw' are in queue and jobs in state 'r' are actively running.
   To check the state of the computer node, type 'qhost.' This command will tell you the cpu, load, and memory use.
3. When doing frequency calculations, typing 'symm=auto' after 'freq' will speed up the calculations.
4. Input files for Opteron must have brackets "{ }" around a command block. For example, this would be acceptable:

```
{rhf;occ,11,5,5,2;wf,45,1,1
}
UCCSD(T)
{freq,symm=auto
thermo,
print,thermo
}
```

However, for Sparc, the brackets are unnecessary and the following would be acceptable:

```
rhf;occ,11,5,5,2;wf,45,1,1

UCCSD(T)

freq,symm=auto
thermo,
print,thermo
```

5. It is necessary to specify the units of Angstrom because the units are in Bohr by default. Type 'ang' on the first line of the geometry and after any variables with the units of Angstroms.
6. The spin symmetry (multiplicity) can be changed using the wave function, 'wf', directive.
7. The error "Unreasonable Norm" can usually be solved be defining the occupied orbitals and the wave function. For example, for HgBr using the Aug-cc-pVTZ-PP basis set, it would be "RHF;occ,11,5,5,2;wf,45,1,1"

8. If optimization of some variables leads to a lower symmetry, i.e. Cs -> C1, it will result in the program dying. Make some changes in your Z-matrix to prevent this.

### B.3 MOLPRO Inputs

**Example 4**: Input file for calculating a single point energy with a given geometry and obtain frequencies and thermodynamics; HgBr at CCSD(T)/Aug-cc-pVTZ level of theory.

Filename: HgBr350.inp

```
***,HgBr r=3.50
memory,24,m
file,1,HgBr350.int
file,2,HgBr350.wfu
print,basis,orbitals
geometry
ang                    !geometry specification, using z-matrix
Hg
Br,Hg,r
end

r=3.50 ang

basis={
!  aug-cc-pVTZ-PP
!
! MERCURY       (11s,10p,9d,3f,2g) -> [6s,6p,5d,3f,2g]
! MERCURY       (10s,9p,8d,2f,1g) -> [5s,5p,4d,2f,1g]
! MERCURY       (1s,1p,1d,1f,1g)
s, HG , 98.3058000, 19.6406000, 12.3397000, 7.7478200, 4.8629100,
1.5771900, 0.7529260, 0.2351120, 0.1039680, 0.0434000, 0.0181000
c, 1.10, 0.0010330, -0.1063820, 0.5320730, -0.5223240, -0.5373210,
0.8847880, 0.5138340, 0.0294070, -0.0061590, 0.0013840
c, 1.10, -0.0003560, 0.0379090, -0.2000130, 0.2240930, 0.1793740, -
0.4508330, -0.3390550, 0.2934140, 0.6446280, 0.2916260
c, 1.10, -0.0002170, -0.0440670, 0.2876950, -0.1894760, -0.7807040,
2.1756040, -0.8865840, -1.8749170, 1.2470530, 0.3523510
c, 1.10, -0.0020930, 0.1557830, -0.7951410, 0.9970540, 0.5928610, -
4.4071970, 5.2898370, -2.8866330, 0.3158740, 0.8226100
c, 10.10, 1.0000000
c, 11.11, 1.0000000
p, HG , 21.4065000, 13.3929000, 6.5102100, 1.8222200, 0.9265070,
0.4550820, 0.1927600, 0.0786890, 0.0317290, 0.0128000
c, 1.9, -0.0128370, 0.0865310, -0.3080410, 0.5327940, 0.4822070,
0.1546950, 0.0132010, 0.0005850, 0.0000200
c, 1.9, 0.0026690, -0.0218770, 0.0865390, -0.1847680, -0.1773950,
0.0009770, 0.3536030, 0.5435820, 0.2455390
c, 1.9, 0.0061400, -0.0480560, 0.1891060, -0.4381190, -0.4321930,
0.4570570, 0.6953570, 0.1420160, 0.0020300
c, 1.9, 0.0130140, -0.0890970, 0.3480200, -1.2184470, 0.1232280,
1.6284380, -0.7824510, -0.5112540, 0.0165110
c, 9.9, 1.0000000
```

```
c, 10.10, 1.0000000
d, HG , 86.9881000, 11.9913000, 6.9364800, 2.0864100, 1.0766400,
0.5311530, 0.2488080, 0.1081700, 0.0470000
c, 1.8, 0.0000580, 0.0127790, -0.0689630, 0.2415630, 0.3878580, 0.3454410,
0.1915090, 0.0465020
c, 1.8, 0.0000500, 0.0192460, -0.1034870, 0.4847690, 0.5069510, -
0.3625720, -0.5729800, -0.1666370
c, 1.8, -0.0000430, 0.0337600, -0.1746100, 1.2017020, -0.5030930, -
1.1299990, 0.7749310, 0.3655340
c, 8.8, 1.0000000
c, 9.9, 1.0000000
f, HG , 1.5814000, 0.5423000, 0.2182000
c, 1.1, 1.0000000
c, 2.2, 1.0000000
c, 3.3, 1.0000000
g, HG , 1.3737000, 0.6361000
c, 1.1, 1.0000000
c, 2.2, 1.0000000

! Effective core Potentials
! -------------------------
ECP, hg, 60, 5 ;
1; !  g-ul potential
2.0000000,1.0000000,0.0000000;
2; !  s-ul potential
2.0000000,12.4130710,275.7747970;
2.0000000,6.8979130,49.2678980;
4; !  p-ul potential
2.0000000,11.3103200,80.5069840;
2.0000000,10.2107730,161.0348240;
2.0000000,5.9398040,9.0834160;
2.0000000,5.0197550,18.3677730;
4; !  d-ul potential
2.0000000,8.4078950,51.1372560;
2.0000000,8.2140860,76.7074590;
2.0000000,4.0126120,6.5618210;
2.0000000,3.7953980,9.8180700;
2; !  f-ul potential
2.0000000,3.2731060,9.4290010;
2.0000000,3.2083210,12.4948560;
2; !  g-ul potential
2.0000000,4.4852960,-6.3384140;
2.0000000,4.5132000,-8.0998630;

! Aug-cc-pVTZ-PP
!
! BROMINE       (11s,12p,10d,2f) -> [6s,5p,4d,2f]
! BROMINE       (10s,11p,9d,1f) -> [5s,4p,3d,1f]
! BROMINE       (1s,1p,1d,1f)
s, BR , 9659.3900000, 1455.9600000, 325.9140000, 46.5657000, 18.2469000,
3.8020100, 1.7863200, 0.6027140, 0.2840140, 0.1202710, 0.0445000
c, 1.7, 0.0003710, 0.0025710, 0.0084850, 0.0782220, -0.3971490, 0.6858640,
0.4868190
c, 1.7, -0.0001520, -0.0010080, -0.0036090, -0.0278720, 0.1513170, -
0.3514970, -0.4107030
```

```
c, 8.8, 1.0000000
c, 9.9, 1.0000000
c, 10.10, 1.0000000
c, 11.11, 1.0000000
p, BR , 492.1870000, 92.3642000, 27.0718000, 7.2653900, 3.4848100,
1.6404800, 0.6485700, 0.2564070, 0.0953040, 0.7666000, 0.1182000,
0.0396000
c, 1.9, 0.0004720, 0.0054940, -0.0880300, 0.3434850, 0.5102080, 0.2486310,
0.0222010, -0.0004190, 0.0006560
c, 1.9, -0.0001580, -0.0013440, 0.0246160, -0.1125320, -0.1797750, -
0.0736610, 0.3487340, 0.5579480, 0.2664560
c, 10.10, 1.0000000
c, 11.11, 1.0000000
c, 12.12, 1.0000000
d, BR , 338.9960000, 103.2170000, 42.3638000, 18.4356000, 8.3725400,
3.8022200, 1.6867700, 0.6775200, 0.2553000, 0.1009000
c, 1.7, 0.0015240, 0.0156730, 0.0724000, 0.1863030, 0.3238810, 0.3745340,
0.2574180
c, 8.8, 1.0000000
c, 9.9, 1.0000000
c, 10.10, 1.0000000
f, BR , 0.5606000, 0.2454000
c, 1.1, 1.0000000
c, 2.2, 1.0000000

! Effective core Potentials
! -------------------------
ECP, br, 10, 4 ;
1; !  g-ul potential
2.0000000,1.0000000,0.0000000;
3; !  s-ul potential
2.0000000,70.0242570,49.9628340;
2.0000000,31.1784120,370.0142050;
2.0000000,7.1565930,10.2414390;
4; !  p-ul potential
2.0000000,46.7734710,99.1122440;
2.0000000,46.1841200,198.2530460;
2.0000000,21.7138580,28.2617400;
2.0000000,20.9417920,56.6233660;
6; !  d-ul potential
2.0000000,50.6988390,-18.6058530;
2.0000000,50.6447640,-27.9232800;
2.0000000,15.4475090,-0.3796930;
2.0000000,15.5002590,-0.7805830;
2.0000000,2.8003910,0.0359680;
2.0000000,1.0774800,0.0943970;
2; !  f-ul potential
2.0000000,14.4656060,-1.0912690;
2.0000000,21.2340650,-2.8876910;
}

{rhf;
occ,11,5,5,2;
wf,45,1,1
}
```

```
UCCSD(T)

{freq,symm=auto
thermo,
print,thermo
}
```

---

**Example 5**: Input file for finding the optimized (lowest energy state) geometry for a molecule and obtaining the frequencies and thermodynamics; HgBr2 at the CCSD(T)/Aug-cc-pVTZ level of theory.

Filename: HgBr2AVTZ.inp

---

```
***,HgBr2 opt
memory,100,m
print,basis,orbitals
r=2.50 ang
geometry
ang
Hg
Br,1,r
Br,1,r,2,180
end


basis={
!  aug-cc-pVTZ-PP
!
! MERCURY       (11s,10p,9d,3f,2g) -> [6s,6p,5d,3f,2g]
! MERCURY       (10s,9p,8d,2f,1g) -> [5s,5p,4d,2f,1g]
! MERCURY       (1s,1p,1d,1f,1g)
s, HG , 98.3058000, 19.6406000, 12.3397000, 7.7478200, 4.8629100,
1.5771900, 0.7529260, 0.2351120, 0.1039680, 0.0434000, 0.0181000
c, 1.10, 0.0010330, -0.1063820, 0.5320730, -0.5223240, -0.5373210,
0.8847880, 0.5138340, 0.0294070, -0.0061590, 0.0013840
c, 1.10, -0.0003560, 0.0379090, -0.2000130, 0.2240930, 0.1793740, -
0.4508330, -0.3390550, 0.2934140, 0.6446280, 0.2916260
c, 1.10, -0.0002170, -0.0440670, 0.2876950, -0.1894760, -0.7807040,
2.1756040, -0.8865840, -1.8749170, 1.2470530, 0.3523510
c, 1.10, -0.0020930, 0.1557830, -0.7951410, 0.9970540, 0.5928610, -
4.4071970, 5.2898370, -2.8866330, 0.3158740, 0.8226100
c, 10.10, 1.0000000
c, 11.11, 1.0000000
p, HG , 21.4065000, 13.3929000, 6.5102100, 1.8222200, 0.9265070,
0.4550820, 0.1927600, 0.0786890, 0.0317290, 0.0128000
c, 1.9, -0.0128370, 0.0865310, -0.3080410, 0.5327940, 0.4822070,
0.1546950, 0.0132010, 0.0005850, 0.0000200
c, 1.9, 0.0026690, -0.0218770, 0.0865390, -0.1847680, -0.1773950,
0.0009770, 0.3536030, 0.5435820, 0.2455390
```

```
c, 1.9, 0.0061400, -0.0480560, 0.1891060, -0.4381190, -0.4321930,
0.4570570, 0.6953570, 0.1420160, 0.0020300
c, 1.9, 0.0130140, -0.0890970, 0.3480200, -1.2184470, 0.1232280,
1.6284380, -0.7824510, -0.5112540, 0.0165110
c, 9.9, 1.0000000
c, 10.10, 1.0000000
d, HG , 86.9881000, 11.9913000, 6.9364800, 2.0864100, 1.0766400,
0.5311530, 0.2488080, 0.1081700, 0.0470000
c, 1.8, 0.0000580, 0.0127790, -0.0689630, 0.2415630, 0.3878580, 0.3454410,
0.1915090, 0.0465020
c, 1.8, 0.0000500, 0.0192460, -0.1034870, 0.4847690, 0.5069510, -
0.3625720, -0.5729800, -0.1666370
c, 1.8, -0.0000430, 0.0337600, -0.1746100, 1.2017020, -0.5030930, -
1.1299990, 0.7749310, 0.3655340
c, 8.8, 1.0000000
c, 9.9, 1.0000000
f, HG , 1.5814000, 0.5423000, 0.2182000
c, 1.1, 1.0000000
c, 2.2, 1.0000000
c, 3.3, 1.0000000
g, HG , 1.3737000, 0.6361000
c, 1.1, 1.0000000
c, 2.2, 1.0000000

! Effective core Potentials
! -------------------------
ECP, hg, 60, 5 ;
1; !  g-ul potential
2.0000000,1.0000000,0.0000000;
2; !  s-ul potential
2.0000000,12.4130710,275.7747970;
2.0000000,6.8979130,49.2678980;
4; !  p-ul potential
2.0000000,11.3103200,80.5069840;
2.0000000,10.2107730,161.0348240;
2.0000000,5.9398040,9.0834160;
2.0000000,5.0197550,18.3677730;
4; !  d-ul potential
2.0000000,8.4078950,51.1372560;
2.0000000,8.2140860,76.7074590;
2.0000000,4.0126120,6.5618210;
2.0000000,3.7953980,9.8180700;
2; !  f-ul potential
2.0000000,3.2731060,9.4290010;
2.0000000,3.2083210,12.4948560;
2; !  g-ul potential
2.0000000,4.4852960,-6.3384140;
2.0000000,4.5132000,-8.0998630;

! Aug-cc-pVTZ-PP
!
! BROMINE       (11s,12p,10d,2f) -> [6s,5p,4d,2f]
! BROMINE       (10s,11p,9d,1f) -> [5s,4p,3d,1f]
! BROMINE       (1s,1p,1d,1f)
```

```
s, BR , 9659.3900000, 1455.9600000, 325.9140000, 46.5657000, 18.2469000,
3.8020100, 1.7863200, 0.6027140, 0.2840140, 0.1202710, 0.0445000
c, 1.7, 0.0003710, 0.0025710, 0.0084850, 0.0782220, -0.3971490, 0.6858640,
0.4868190
c, 1.7, -0.0001520, -0.0010080, -0.0036090, -0.0278720, 0.1513170, -
0.3514970, -0.4107030
c, 8.8, 1.0000000
c, 9.9, 1.0000000
c, 10.10, 1.0000000
c, 11.11, 1.0000000
p, BR , 492.1870000, 92.3642000, 27.0718000, 7.2653900, 3.4848100,
1.6404800, 0.6485700, 0.2564070, 0.0953040, 0.7666000, 0.1182000,
0.0396000
c, 1.9, 0.0004720, 0.0054940, -0.0880300, 0.3434850, 0.5102080, 0.2486310,
0.0222010, -0.0004190, 0.0006560
c, 1.9, -0.0001580, -0.0013440, 0.0246160, -0.1125320, -0.1797750, -
0.0736610, 0.3487340, 0.5579480, 0.2664560
c, 10.10, 1.0000000
c, 11.11, 1.0000000
c, 12.12, 1.0000000
d, BR , 338.9960000, 103.2170000, 42.3638000, 18.4356000, 8.3725400,
3.8022200, 1.6867700, 0.6775200, 0.2553000, 0.1009000
c, 1.7, 0.0015240, 0.0156730, 0.0724000, 0.1863030, 0.3238810, 0.3745340,
0.2574180
c, 8.8, 1.0000000
c, 9.9, 1.0000000
c, 10.10, 1.0000000
f, BR , 0.5606000, 0.2454000
c, 1.1, 1.0000000
c, 2.2, 1.0000000

! Effective core Potentials
! -------------------------
ECP, br, 10, 4 ;
1; !  g-ul potential
2.0000000,1.0000000,0.0000000;
3; !  s-ul potential
2.0000000,70.0242570,49.9628340;
2.0000000,31.1784120,370.0142050;
2.0000000,7.1565930,10.2414390;
4; !  p-ul potential
2.0000000,46.7734710,99.1122440;
2.0000000,46.1841200,198.2530460;
2.0000000,21.7138580,28.2617400;
2.0000000,20.9417920,56.6233660;
6; !  d-ul potential
2.0000000,50.6988390,-18.6058530;
2.0000000,50.6447640,-27.9232800;
2.0000000,15.4475090,-0.3796930;
2.0000000,15.5002590,-0.7805830;
2.0000000,2.8003910,0.0359680;
2.0000000,1.0774800,0.0943970;
2; !  f-ul potential
2.0000000,14.4656060,-1.0912690;
2.0000000,21.2340650,-2.8876910;
```

```
}

HF

CCSD(T)
optg

{freq,symm=auto
thermo,
print,thermo}

show,r
```

---

**Example 6**: Input file for obtaining thermodynamics and partition functions at different temperatures using the integral and wave function files from Example 1.

Filename: HgBr350t.inp

---

```
***,HgBr r=3.50
memory,24,m
file,1,HgBr350.int
file,2,HgBr350.wfu
goto,freq
geometry
ang                    !geometry specification, using z-matrix
Hg
Br,Hg,r
end

r=3.50 ang

basis={
!  aug-cc-pVTZ-PP
!
! MERCURY       (11s,10p,9d,3f,2g) -> [6s,6p,5d,3f,2g]
! MERCURY       (10s,9p,8d,2f,1g) -> [5s,5p,4d,2f,1g]
! MERCURY       (1s,1p,1d,1f,1g)
s, HG , 98.3058000, 19.6406000, 12.3397000, 7.7478200, 4.8629100,
1.5771900, 0.7529260, 0.2351120, 0.1039680, 0.0434000, 0.0181000
c, 1.10, 0.0010330, -0.1063820, 0.5320730, -0.5223240, -0.5373210,
0.8847880, 0.5138340, 0.0294070, -0.0061590, 0.0013840
c, 1.10, -0.0003560, 0.0379090, -0.2000130, 0.2240930, 0.1793740, -
0.4508330, -0.3390550, 0.2934140, 0.6446280, 0.2916260
c, 1.10, -0.0002170, -0.0440670, 0.2876950, -0.1894760, -0.7807040,
2.1756040, -0.8865840, -1.8749170, 1.2470530, 0.3523510
c, 1.10, -0.0020930, 0.1557830, -0.7951410, 0.9970540, 0.5928610, -
4.4071970, 5.2898370, -2.8866330, 0.3158740, 0.8226100
c, 10.10, 1.0000000
c, 11.11, 1.0000000
p, HG , 21.4065000, 13.3929000, 6.5102100, 1.8222200, 0.9265070,
0.4550820, 0.1927600, 0.0786890, 0.0317290, 0.0128000
```

```
c, 1.9, -0.0128370, 0.0865310, -0.3080410, 0.5327940, 0.4822070,
0.1546950, 0.0132010, 0.0005850, 0.0000200
c, 1.9, 0.0026690, -0.0218770, 0.0865390, -0.1847680, -0.1773950,
0.0009770, 0.3536030, 0.5435820, 0.2455390
c, 1.9, 0.0061400, -0.0480560, 0.1891060, -0.4381190, -0.4321930,
0.4570570, 0.6953570, 0.1420160, 0.0020300
c, 1.9, 0.0130140, -0.0890970, 0.3480200, -1.2184470, 0.1232280,
1.6284380, -0.7824510, -0.5112540, 0.0165110
c, 9.9, 1.0000000
c, 10.10, 1.0000000
d, HG , 86.9881000, 11.9913000, 6.9364800, 2.0864100, 1.0766400,
0.5311530, 0.2488080, 0.1081700, 0.0470000
c, 1.8, 0.0000580, 0.0127790, -0.0689630, 0.2415630, 0.3878580, 0.3454410,
0.1915090, 0.0465020
c, 1.8, 0.0000500, 0.0192460, -0.1034870, 0.4847690, 0.5069510, -
0.3625720, -0.5729800, -0.1666370
c, 1.8, -0.0000430, 0.0337600, -0.1746100, 1.2017020, -0.5030930, -
1.1299990, 0.7749310, 0.3655340
c, 8.8, 1.0000000
c, 9.9, 1.0000000
f, HG , 1.5814000, 0.5423000, 0.2182000
c, 1.1, 1.0000000
c, 2.2, 1.0000000
c, 3.3, 1.0000000
g, HG , 1.3737000, 0.6361000
c, 1.1, 1.0000000
c, 2.2, 1.0000000

! Effective core Potentials
! -------------------------
ECP, hg, 60, 5 ;
1; !  g-ul potential
2.0000000,1.0000000,0.0000000;
2; !  s-ul potential
2.0000000,12.4130710,275.7747970;
2.0000000,6.8979130,49.2678980;
4; !  p-ul potential
2.0000000,11.3103200,80.5069840;
2.0000000,10.2107730,161.0348240;
2.0000000,5.9398040,9.0834160;
2.0000000,5.0197550,18.3677730;
4; !  d-ul potential
2.0000000,8.4078950,51.1372560;
2.0000000,8.2140860,76.7074590;
2.0000000,4.0126120,6.5618210;
2.0000000,3.7953980,9.8180700;
2; !  f-ul potential
2.0000000,3.2731060,9.4290010;
2.0000000,3.2083210,12.4948560;
2; !  g-ul potential
2.0000000,4.4852960,-6.3384140;
2.0000000,4.5132000,-8.0998630;

! Aug-cc-pVTZ-PP
!
```

```
! BROMINE       (11s,12p,10d,2f) -> [6s,5p,4d,2f]
! BROMINE       (10s,11p,9d,1f) -> [5s,4p,3d,1f]
! BROMINE       (1s,1p,1d,1f)
s, BR , 9659.3900000, 1455.9600000, 325.9140000, 46.5657000, 18.2469000,
3.8020100, 1.7863200, 0.6027140, 0.2840140, 0.1202710, 0.0445000
c, 1.7, 0.0003710, 0.0025710, 0.0084850, 0.0782220, -0.3971490, 0.6858640,
0.4868190
c, 1.7, -0.0001520, -0.0010080, -0.0036090, -0.0278720, 0.1513170, -
0.3514970, -0.4107030
c, 8.8, 1.0000000
c, 9.9, 1.0000000
c, 10.10, 1.0000000
c, 11.11, 1.0000000
p, BR , 492.1870000, 92.3642000, 27.0718000, 7.2653900, 3.4848100,
1.6404800, 0.6485700, 0.2564070, 0.0953040, 0.7666000, 0.1182000,
0.0396000
c, 1.9, 0.0004720, 0.0054940, -0.0880300, 0.3434850, 0.5102080, 0.2486310,
0.0222010, -0.0004190, 0.0006560
c, 1.9, -0.0001580, -0.0013440, 0.0246160, -0.1125320, -0.1797750, -
0.0736610, 0.3487340, 0.5579480, 0.2664560
c, 10.10, 1.0000000
c, 11.11, 1.0000000
c, 12.12, 1.0000000
d, BR , 338.9960000, 103.2170000, 42.3638000, 18.4356000, 8.3725400,
3.8022200, 1.6867700, 0.6775200, 0.2553000, 0.1009000
c, 1.7, 0.0015240, 0.0156730, 0.0724000, 0.1863030, 0.3238810, 0.3745340,
0.2574180
c, 8.8, 1.0000000
c, 9.9, 1.0000000
c, 10.10, 1.0000000
f, BR , 0.5606000, 0.2454000
c, 1.1, 1.0000000
c, 2.2, 1.0000000

! Effective core Potentials
! -------------------------
ECP, br, 10, 4 ;
1; !  g-ul potential
2.0000000,1.0000000,0.0000000;
3; !  s-ul potential
2.0000000,70.0242570,49.9628340;
2.0000000,31.1784120,370.0142050;
2.0000000,7.1565930,10.2414390;
4; !  p-ul potential
2.0000000,46.7734710,99.1122440;
2.0000000,46.1841200,198.2530460;
2.0000000,21.7138580,28.2617400;
2.0000000,20.9417920,56.6233660;
6; !  d-ul potential
2.0000000,50.6988390,-18.6058530;
2.0000000,50.6447640,-27.9232800;
2.0000000,15.4475090,-0.3796930;
2.0000000,15.5002590,-0.7805830;
2.0000000,2.8003910,0.0359680;
2.0000000,1.0774800,0.0943970;
```

```
2; !  f-ul potential
2.0000000,14.4656060,-1.0912690;
2.0000000,21.2340650,-2.8876910;
}

{rhf;
occ,11,5,5,2;
wf,45,1,1
}

UCCSD(T)

{freq,read=5300.2
thermo,
print,thermo
temp,600,2000,100
}
```

---

**Example 7**: Input file for building a PES for HgCl decomposition reaction at the CCSD(T)/Aug-cc-pVTZ level of theory.

Filename: HgClPES.inp

---

```
***,HgCl opt
memory,25,m
print,basis,orbitals
geometry                    !geometry specification, using z-matrix
Ang
Hg
Cl,Hg,r(i)
end

distances=[2.25,2.50,2.75,3.00,3.25,3.50,3.75,4.0,4.25,4.50,4.75] ang

basis={
!
! MERCURY       (11s,10p,9d,3f,2g) -> [6s,6p,5d,3f,2g]
! MERCURY       (10s,9p,8d,2f,1g) -> [5s,5p,4d,2f,1g]
! MERCURY       (1s,1p,1d,1f,1g)
s, HG , 98.3058000, 19.6406000, 12.3397000, 7.7478200, 4.8629100,
1.5771900, 0.7529260, 0.2351120, 0.1039680, 0.0434000, 0.0181000
c, 1.10, 0.0010330, -0.1063820, 0.5320730, -0.5223240, -0.5373210,
0.8847880, 0.5138340, 0.0294070, -0.0061590, 0.0013840
c, 1.10, -0.0003560, 0.0379090, -0.2000130, 0.2240930, 0.1793740, -
0.4508330, -0.3390550, 0.2934140, 0.6446280, 0.2916260
c, 1.10, -0.0002170, -0.0440670, 0.2876950, -0.1894760, -0.7807040,
2.1756040, -0.8865840, -1.8749170, 1.2470530, 0.3523510
c, 1.10, -0.0020930, 0.1557830, -0.7951410, 0.9970540, 0.5928610, -
4.4071970, 5.2898370, -2.8866330, 0.3158740, 0.8226100
c, 10.10, 1.0000000
c, 11.11, 1.0000000
```

```
p, HG , 21.4065000, 13.3929000, 6.5102100, 1.8222200, 0.9265070,
0.4550820, 0.1927600, 0.0786890, 0.0317290, 0.0128000
c, 1.9, -0.0128370, 0.0865310, -0.3080410, 0.5327940, 0.4822070,
0.1546950, 0.0132010, 0.0005850, 0.0000200
c, 1.9, 0.0026690, -0.0218770, 0.0865390, -0.1847680, -0.1773950,
0.0009770, 0.3536030, 0.5435820, 0.2455390
c, 1.9, 0.0061400, -0.0480560, 0.1891060, -0.4381190, -0.4321930,
0.4570570, 0.6953570, 0.1420160, 0.0020300
c, 1.9, 0.0130140, -0.0890970, 0.3480200, -1.2184470, 0.1232280,
1.6284380, -0.7824510, -0.5112540, 0.0165110
c, 9.9, 1.0000000
c, 10.10, 1.0000000
d, HG , 86.9881000, 11.9913000, 6.9364800, 2.0864100, 1.0766400,
0.5311530, 0.2488080, 0.1081700, 0.0470000
c, 1.8, 0.0000580, 0.0127790, -0.0689630, 0.2415630, 0.3878580, 0.3454410,
0.1915090, 0.0465020
c, 1.8, 0.0000500, 0.0192460, -0.1034870, 0.4847690, 0.5069510, -
0.3625720, -0.5729800, -0.1666370
c, 1.8, -0.0000430, 0.0337600, -0.1746100, 1.2017020, -0.5030930, -
1.1299990, 0.7749310, 0.3655340
c, 8.8, 1.0000000
c, 9.9, 1.0000000
f, HG , 1.5814000, 0.5423000, 0.2182000
c, 1.1, 1.0000000
c, 2.2, 1.0000000
c, 3.3, 1.0000000
g, HG , 1.3737000, 0.6361000
c, 1.1, 1.0000000
c, 2.2, 1.0000000

! Effective core Potentials
! -------------------------
ECP, hg, 60, 5 ;
1; !  g-ul potential
2.0000000,1.0000000,0.0000000;
2; !  s-ul potential
2.0000000,12.4130710,275.7747970;
2.0000000,6.8979130,49.2678980;
4; !  p-ul potential
2.0000000,11.3103200,80.5069840;
2.0000000,10.2107730,161.0348240;
2.0000000,5.9398040,9.0834160;
2.0000000,5.0197550,18.3677730;
4; !  d-ul potential
2.0000000,8.4078950,51.1372560;
2.0000000,8.2140860,76.7074590;
2.0000000,4.0126120,6.5618210;
2.0000000,3.7953980,9.8180700;
2; !  f-ul potential
2.0000000,3.2731060,9.4290010;
2.0000000,3.2083210,12.4948560;
2; !  g-ul potential
2.0000000,4.4852960,-6.3384140;
2.0000000,4.5132000,-8.0998630;
```

```
! Aug-cc-pVTZ
! CHLORINE       (12s,8p,1d)->[4s,3p,1d]
! CHLORINE       (1s,1p,1d)
! CHLORINE       (1s,1p,1d)
s, CL , 127900., 19170., 4363., 1236., 403.6, 145.7, 56.81, 23.23, 6.644,
2.575, 0.5371, 0.1938, 8.273, 0.06080
c, 1.11, 0.241153D-03, 0.187095D-02, 0.970827D-02, 0.393153D-01,
0.125932D+00, 0.299341D+00, 0.421886D+00, 0.237201D+00, 0.191531D-01, -
0.334792D-02, 0.929883D-03
c, 1.11, -0.678922D-04, -0.521836D-03, -0.276513D-02, -0.111537D-01, -
0.385919D-01, -0.994848D-01, -0.201392D+00, -0.130313D+00, 0.509443D+00,
0.610725D+00, 0.421549D-01
c, 1.11, 0.204986D-04, 0.158298D-03, 0.833639D-03, 0.339880D-02,
0.116738D-01, 0.309622D-01, 0.629533D-01, 0.460257D-01, -0.219312D+00, -
0.408773D+00, 0.638465D+00
c, 12.12, 1.0
c, 13.13, 1.000000
c, 14.14, 1.000000
p, CL , 417.6, 98.33, 31.04, 11.19, 4.249, 1.624, 0.5322, 0.1620, 3.697,
0.04660
c, 1.7, 0.525982D-02, 0.398332D-01, 0.164655D+00, 0.387322D+00,
0.457072D+00, 0.151636D+00, 0.181615D-02
c, 1.7, -0.143570D-02, -0.107796D-01, -0.470075D-01, -0.111030D+00, -
0.153275D+00, 0.894609D-01, 0.579444D+00
c, 8.8, 1.0
c, 9.9, 1.000000
c, 10.10, 1.000000
d, CL , 0.60000, 9.844, 0.19600
c, 1.1, 1.000000
c, 2.2, 1.000000
c, 3.3, 1.000000
}

i=0
do ir=1,#distances
i=i+1
r(i)=distances(ir)
RHF;occ,10,4,4,1;wf,37,1,1
escf(i)=energy
UCCSD(T)
euccsdt(i)=energy

enddo

table,r,escf,euccsdt
head, r,scf,uccsd(t)
save,HgClPES.tab
title, Results for HgCl PES, basis $basis
```

---

## B.4 MOLPRO Outputs

**Table B1**. Output values from Examples 4 & 5 needed for reaction kinetics calculation. (Energies are in hartrees/particle.)

| | HgBr | $HgBr_2$ |
|---|---|---|
| **Level of Theory** | CCSD(T)/Aug-cc-pVTZ | CCSD(T)/Aug-cc-pVTZ |
| **Geometry (Å)** | 3.25 | 2.4 (optimized) |
| | | 180 |
| **Ground State Energy** | -568.6368469 | -5298.332946 |
| **Enthalpy @ 298K** | -568.633542 | -5298.327517 |
| **Frequenc(ies)** | -56.19 | 219.1600 |
| | -- | 290.3000 |
| | -- | 69.8400 |
| | **Partition Coefficients (Q)** | |
| **Electronic** | 2 | 1 |
| **Translational** | 1.85E+08 | 2.69E+08 |
| **Rotational** | 8.60E+03 | 1.13E+04 |

**Table B2**. Ouput values from Example 6 needed for reaction kinetics calculation.

| Temperature | Enthalpy | Partition Coefficients (Q) | | |
|---|---|---|---|---|
| (K) | (Hartree/particle) | Electronic | Translational | Rotational |
| 700 | -568.629088 | 2 | 1.56E+09 | 2.02E+04 |
| 1000 | -568.625763 | 2 | 3.80E+09 | 2.89E+04 |
| 1500 | -568.620221 | 2 | 1.05E+10 | 4.33E+04 |
| 2000 | -568.614679 | 2 | 2.15E+10 | 5.77E+04 |

**Table B3**. Output values from Example 7 for HgCl PES. (Energies are in hatrees/particle.)

| r (Å) | SCF | UCCSD(T) |
|---|---|---|
| 2.25 | -612.0311409 | -612.621012 |
| 2.50 | -612.0351839 | -612.6240699 |
| 2.75 | -612.0225444 | -612.6149264 |
| 3.00 | -612.0059271 | -612.6060586 |
| 3.25 | -611.9942195 | -612.6005907 |
| 3.50 | -611.9716565 | -612.5960521 |
| 3.75 | -611.9612817 | -612.5950072 |
| 4.00 | -611.9637643 | -612.5955087 |
| 4.25 | -611.9579037 | -612.5938077 |
| 4.50 | -612.0093047 | -612.5950236 |
| 4.75 | -612.0093276 | -612.5948255 |

# Bibliography


1. United States Environmental Protection Agency, 2005 Clean Air Interstate Rule. http://www.epa.gov/interstateairquality (accessed July 2008).

2. Vosteen, B. W.; Kanefke, R.; Koser, H. *VGB PowerTech* **2006**, *86*, 70.

3. Liu, S.; Yan, N.; Liu, Z.; Qu, Z.; Wang, H. P.; Chang, S.; Miller, C. *Environ. Sci. Technol.* **2007**, *41*, 1405.
4. U. S. Environmental Protection Agency, Clean Air Mercury Rule. http://www.epa.gov/oar/mercuryrule/index.htm (accessed January 2007).

5. United States Environmental Protection Agency 2002. Results of 1999 Information Collection Request. http://www.epa.gov/ttn/atw/combust/utiltox/icrdata.xls (accessed June 2007).

6. Senior, C. L.; Helble, J. J.; Sarofim, A. F. Fuel Process. Technol. **2000**, *65-66*, 263.

7. Gaussian 03, Revision 6.0, Frisch, M. J.; Trucks, G. W.; Schlegel, H. B.; Scuseria, G. E.; Robb, M. A.; Cheeseman, J. R.; Montgomery, Jr., J. A.; Vreven, T.; Kudin, K. N.; Burant, J. C.; Millam, J. M.; Iyengar, S. S.; Tomasi, J.; Barone, V.; Mennucci, B.; Cossi, M.; Scalmani, G.; Rega, N.; Petersson, G. A.; Nakatsuji, H.; Hada, M.; Ehara, M.; Toyota, K.; Fukuda, R.; Hasegawa, J.; Ishida, M.; Nakajima, T.; Honda, Y.; Kitao, O.; Nakai, H.; Klene, M.; Li, X.; Knox, J. E.; Hratchian, H. P.; Cross, J. B.; Bakken, V.; Adamo, C.; Jaramillo, J.; Gomperts, R.; Stratmann, R. E.; Yazyev, O.; Austin, A. J.; Cammi, R.; Pomelli, C.; Ochterski, J. W.; Ayala, P. Y.; Morokuma, K.; Voth, G. A.; Salvador, P.; Dannenberg, J. J.; Zakrzewski, V. G.; Dapprich, S.; Daniels, A. D.; Strain, M. C.; Farkas, O.; Malick, D. K.; Rabuck, A. D.; Raghavachari, K.; Foresman, J. B.; Ortiz, J. V.; Cui, Q.; Baboul, A. G.; Clifford, S.; Cioslowski, J.; Stefanov, B. B.; Liu, G.; Liashenko, A.; Piskorz, P.; Komaromi, I.; Martin, R. L.; Fox, D. J.; Keith, T.; Al-Laham, M. A.; Peng, C. Y.; Nanayakkara, A.; Challacombe, M.; Gill, P. M. W.; Johnson, B.; Chen, W.; Wong, M. W.; Gonzalez, C.; and Pople, J. A.; Gaussian, Inc., Wallingford CT, 2004.

8. MOLPRO, version 2002.6 is a package of ab initio programs written by Werner, H. J. and Knowles, P. J. with contributions from Almlöf, J.; Amos, R. D.; Berning, A.; Cooper, D. L.; Deegan, M. J. O.; Dobbyn, A. J.; Eckert, F.; Elbert, S. T.; Hampel, C.; Lindh, R.; Lloyd, A. W.; Meyer, W.; Nicklass, A.; Peterson, K.; Pitzer, R.; Stone, A. J.; Taylor, P. R.; Mura, M. E.; Pulay, P.; Schütz, M.; Stoll, H.; Thorsteinsson, T.

9. Holbrook, K.A.; Pilling, M.J.; Robertson, S.H. *Unimolecular Reactions*, 2nd Edition; Wiley: New York, 1996.

10. Lipson, R. H.; Jordan, K. J.; Bascal, H. A. *J. Chem. Phys.* **1993**, *98*, 959.

11. Deyanov, R. Z.; Petrov, K. P.; Ugarov, V. V.; Shchedrin, B. M.; Rambidi, N. G. *Zh. Strukt. Khimii* **1985**, *26*, 58.

12. Focsa, C.; Li, H.; Bernath, P. F. *J. Mol. Spectrosc.* **2000**, *200*, 104.

13. Givan, A.; Loewenschuss, A. *J. Mol. Spectrosc.* **1978**, *48*, 325.

14. Cundari, T. R.; Yoshikawa, A. *J. Comput. Chem.* **1998**, *19*, 902.

15. Goodsite, M. E.; Plane, J. M. C.; Skov, H. *Environ. Sci. Technol.* **2004**, *38*, 1772.

16. Shepler, B. C.; Balabanov, N. B.; Peterson, K. A. *J. Chem. Phys.* **2007**, *127*, 164304.

17. Huber, K. P.; Herzberg, G. *Molecular Spectra and Molecular Structure IV. Constants of Diatomic Molecules;* Van Nostrand: Princeton, NJ, 1979.

18. Nishimiya, N.; Yukiya, T.; Ohtsuka, T.; Suzuki, M. *J. Mol. Spectrosc.* **1997**, *182*, 309.

19. Tellinghuisen, J.; Ashmore, J. G. *Appl. Phys. Lett.* **1982**, *40*, 867.

20. Beattie, I. R.; Horder, J. R.; Jones, P. J. *J. Chem. Soc. A* **1970**, 329.

21. Malt'sev, A. A.; Selivanov, G. K.; Yampolsky, V. I.; Zavalishin, N. I. *Nature: Physical Science* **1971**, *231*, 157.

22. Klemperer, W.; Lindeman, L. *J. Chem. Phys.* **2004**, *25*, 397.

23. Chase, M. W. NIST-JANAF Thermochemical Tables. **1998**, *1*, 1952.

24. Cox, J. D.; Wagman, D. D.; Medvedev, V. A. *CODATA key values for thermodynamics*, Hemisphere Publishing Company: New York, 1989.

25. Balabanov, N. B.; Peterson, K. *J. Phys. Chem. A* **2003**, *107*, 7465.

26. Greig, G.; Gunning, H. E.; Strausz, O. P. *J Chem. Phys.* **1970**, *52*, 3684.

27. Ariya, P.A.; Khalizov, A.; Gidas, A. *J. Phys. Chem. A* **2002**, *106*, 7310.

28. Spicer, C. W.; Satola, J.; Abbgy, A. A.; Plastridge, R. A.; Cowen, K. *Florida Department of Environmental Protection*: 2002.

29. Donohoue, D. L.; Bauer, D.; Cossairt, B. ; Hynes, A. J. *J. Phys. Chem. A* **2006**, *110*, 6623.

30. Khalizov, A. F.; Viswanathan, B.; Larregaray, P.; Ariya, P. A. *J. Phys. Chem. A* **2003**, *107*, 6360.

31. Goodsite, M. E.; Plane, J. M. C.; Skov, H. *Environ. Sci. Technol.* **2004**, *38*, 1772.

32. Balabanov, N.B.; Shepler, B. C.; Peterson, K. A. *J. Phys. Chem. A* **2005**, *109*, 8765.

33. Eyring, H. *J. Chem. Phys.* **1935**, *3*, 107.

34. Becke, A. D. *J.Chem.Phys.* **1993**, *98*, 5648.

35. Stephens, P. J.; Devlin, F. J.; Chabalowski, C. F., Frisch, M. J. *J.Phys.Chem.* **1994**, *98*, 11623.

36. Knowles, P. J.; Werner, H. J. *Chem. Phys. Lett.* **1988**, *145* (6), 514.

37. Werner, H. J.; Knowles, P. J. *J. Chem. Phys.* **1988**, *89*, 5803.

38. Langhoff, S. R.; Davidson, E. R. *Int. J. Quantum Chem.* **1974**, *8*, 61.

39. Blomberg, M. R. A.; Siegbahn, P. E. M. *J. Chem. Phys.* **1983**, *78*, 5682.

40. Simons, J. *J. Phys. Chem.* **1989**, *93*, 626.

41. Hay, P. J.; Wadt, W. R. *J. Chem. Phys.* **1985**, *82*, 299.

42. Stevens, W. J.; Krauss, M. *Can. J. Chem.* **1992**, *70*, 612.

43. Peterson, K. A.; Puzzarini, C. *Theor. Chem. Acc.* **2005**, *114*, 283.

44. Peterson, K. A.; Figgen, D.; Goll, E.; Stoll, H.; Dolg, M. *J. Chem. Phys.* **2003**, *119*(21), 11113.

45. Figgen, D.; Rauhut, G.; Dolg, M.; Stoll, H. *Chem. Phys.* **2005**, *311*, 227.

46. Coxon, J. A.; Hajigeorgiou, P. G. *J. Mol. Spectrosc.* **1991**, *150*, 1.

47. Huber, K. P.; Herzberg, G. *Molecular Spectra and Molecular Structure IV. Constants of Diatomic Molecules;* Van Nostrand: Princeton, NJ, 1979.

48. Focsa, C.; Li, H.; Bernath, P. F. *J. Mol. Spectrosc.* **2000**, *200*, 104.

49. Nishimiya, N.; Yukiya, T.; Ohtsuka, T.; Suzuki, M. *J. Mol. Spectrosc.* **1997**, *182*, 309.

50. Malt'sev, A. A.; Selivanov, G. K.; Yampolsky, V. I.; Zavalishin, N. I. *Nature: Physical Science* **1971**, *231*, 157.

51. Shepler, B. C.; Balabanov, N. B.; Peterson, K. A. *J. Phys. Chem. A* **2005**, *109*, 10363.

52. Stein, S.E. IR and Mass Spectra. *NIST Chemistry WebBook;* Mallard, W.G.; Linstrom, P.J., Eds. NIST Standard Reference Database Number 69; National Institute of Standards and Technology: Gaithersburg, MD, (February) 2000, 1,2-Ethanediol (http://webbook.nist.gov).

53. Lide, David R., Ed. *CRC Handbook of Chemistry and Physics;* Taylor and Francis: Boca Raton, FL, 2007; Vol. Internet Version 2007.

54. Wilmouth, D. M.; Hanisco, T. F.; Donahue, N. M.; Anderson, J. G. *J. Phys. Chem. A* **1999**, *103*, 8935.

55. Riedel, S.; Straka, M.; Kaupp, M. *Phys. Chem. Chem. Phys.* **2004**, *6*, 1122.

56. Vosko, S. J.; Wilk, L.; Nusair, M. *Can. J. Phys.* **1980**, *58*, 1200.

57. Becke, A. D. *Phys. Rev. A* **1988**, *38*, 3098.

58. Perdew, J. P. *Phys. Rev. B* **1986**, *33*, 8822.

59. Aylett, B. J. *Comprehensive Inorganic Chemistry;* Pergamon Press: Elmsford, NY, 1973; Vol. 3.

60. Gregg, A. H.; Hampson, G. C.; Jenkins, G. I.; Jones, P. L. F.; Sutton, L. E. *Trans. Faraday Soc.* **1937**, *33*, 852.

61. Wigner, E. *Z. Phys. Chem. B* **1932**, *19*, 203.

62. Gilbert, R. G.; Smith, S. C. *Theory of Unimolecular Reactions*; Blackwell Scientific Publications: Oxford, 1990.

63. Reid, R.C.; Prausnitz, J.M.; Poling, B.E. *The Properties of Gases and Liquids*; McGraw Hill Companies: 4th Edition, April 1987.

64. Deyanov, R. Z.; Petrov, K. P.; Ugarov, V. V.; Shchedrin, B. M.; Rambidi, N. G. *Zh. Strukt. Khimii* **1985**, *26*, 58.

65. Fishtik, Ilie; Callaghan, Caitlin A.; Datta, Ravindra. *J. Phys. Chem. B* **2004**, *108(18)*, 5671.